

ICTHYOPLANKTONIC VERTICAL DISTRIBUTION & INGRESS
IN THE ARANSAS PASS INLET SYSTEM

A Thesis

by

OLIVIA A. ROBSON

BS, University of Connecticut, 2016

Submitted in Partial Fulfillment of the Requirements for the Degree of

MASTER OF SCIENCE

in

BIOLOGY

Texas A&M University-Corpus Christi
Corpus Christi, Texas

December 2023

© Olivia Ann Robson

All Rights Reserved

December 2023

ICTHYOPLANKTONIC VERTICAL DISTRIBUTION & INGRESS
IN THE ARANSAS PASS INLET SYSTEM

A Thesis

by

OLIVIA A. ROBSON

This thesis meets the standards for scope and quality of
Texas A&M University-Corpus Christi and is hereby approved.

David Portnoy, PhD
Chair

James Tolan, PhD
Committee Member

Kim Withers, PhD
Committee Member

December 2023

ABSTRACT

In the Coastal Bend region of Texas desalination plants have been proposed as a solution to water usage problems. These plants take in brackish/marine water and dispose of brine, which in coastal inlets would create a plume of water with higher salinity and temperature. Desalination plants could impact estuarine dependent fishes whose larvae pass through the inlets on their way to nursery habitat. In this study I sample the Aransas Pass Inlet system, in the vicinity of one of the proposed desalination plans, during day and night and during both incoming and outgoing tides at three different depth strata, to provide data on larval assemblages in the channel. Results showed that larval were greatest in the deepest stratum and during nighttime hours. Key spawning months for several important families were also confirmed. Briny discharge may adversely affect larval development and survival depending on sensitivity to abrupt changes in salinity and temperature, which differs by species and developmental stage. Currently there are no specific regulations addressing desalination plant discharge, but this research suggests those regulations should limit the location and timing of discharge to mitigate potential negative impacts on local ichthyofauna.

DEDICATION

Dedicated to my two biggest supports Wendy and Kyle, for always encouraging me to chase after my dreams.

ACKNOWLEDGEMENTS

I would like to thank my committee members for their expert knowledge and guidance. I would also like to thank Dr. Blair Sterba-Boatright for his assistance with all statistical analysis, Dr. Shannan McCaskill for her help and support throughout the entire process, Dr Simon Geist for his guidance, and all undergraduate volunteers who helped in field. Finally, I would like to thank my funding sources at the Coastal Bend and Bays Estuarine Program and the TAMUCC Department of Life Sciences.

TABLE OF CONTENTS

	Page
ABSTRACT.....	iv
DEDICATION.....	v
ACKNOWLEDGEMENTS.....	vi
TABLE OF CONTENTS.....	vii
LIST OF FIGURES.....	x
LIST OF TABLES.....	xii
1. INTRODUCTION.....	1
1.1. Passive Transport of Larval Planktonic Organisms.....	2
1.2. Active Transport of Larval Planktonic Organisms.....	3
1.3. Larval Transport though the Aransas Pass Inlet System.....	5
1.4. Potential effects of desalination brine plume on larval health & survival.....	6
1.5. Objectives and Hypothesis.....	8
2. MATERIALS & METHODS.....	9
2.1. Study Site.....	9
2.2. Sampling Design.....	9
2.3. Water Quality Measurements.....	11
2.4. Plankton Sample Collection & Processing.....	11
2.5. Ichthyoplankton Community Analysis.....	13
2.5.1. Total Density.....	13
2.6. Ichthyoplankton Transport Comparisons.....	13
2.6.1. Family Level Diversity.....	13

2.6.2. PCA.....	14
2.6.3. Sciaenid Species Density	14
2.6.4. Paralichthyidae Family	14
3. RESULTS	16
3.1. Water Quality.....	16
3.1.1. June & July	17
3.1.2. October.....	18
3.1.3. November.....	19
3.1.4. February	19
3.1.5. September.....	19
3.2. Community Composition	20
3.2.1. Family Composition.....	20
3.2.2. Sciaenidae Species Composition	26
3.2.3. Paralichthyid Barcoding Results.....	29
3.3. Total Larval Density Community Analysis	30
3.3.1. Day Model.....	30
3.3.2. Night Model.....	30
3.4. Family Density Analysis	35
3.4.1. Sciaenidae	35
3.5. Family PCA	38
4. DISCUSSION.....	46
4.1. Ichthyoplankton Community	46
4.2. Ichthyoplankton Transportation.....	47

4.3. Implications for management: Possible environmental effects	50
4.4. Summary & Conclusions	51
REFERENCES	53
APPENDIX: STATION CODE DEFINITIONS.....	62

LIST OF FIGURES

	Page
Figure 1. Conceptual model displaying the response of three taxa (<i>Leiostomus xanthurus</i> , <i>Micropogonias undulatus</i> , and <i>Paralichthys</i> spp.) of ichthyoplankton to photoperiod and tidal flow.....	5
Figure 2. Map of sampling area in coastal Texas displaying sampling sites Corpus Christi Channel, Aransas Pass Channel, Lydia Ann Channel, and Port Aransas (CC1, AP1, LA1, & PA1 respectively).....	11
Figure 3. Depth profiles of temperature (° C) on the left-hand side and salinity on the right-hand side arranged by sampling month.	17
Figure 4. Depth profile of dissolved oxygen (DO) concentrations (mg/L) for sampling stations Corpus Christi night in (CCNI), Aransas Pass night in (AP1NI), Port Aransas night in (PA1NI), and Port Aransas day in (PA1DOI) taken during June.	18
Figure 5. Data provided by NOAA (bouy station RTAT2) of surface water temperatures in the Corpus Christi Channel for the sample date of September 11 th , 2022.....	20
Figure 6. Median total ichthyoplankton densities (fish/ 100m ³) captured during the day (grey) and night (purple) for September, October, November, and February.	31
Figure 7. Median total ichthyoplankton densities (fish/ 100m ³) captured during ingoing tide (green) and outgoing tide (orange) for samples collected during the day.	33
Figure 8. Median total ichthyoplankton densities (fish/ 100m ³) captured at surface depths (red) and non-surface depths (blue; ns) for samples collected during the night.....	34
Figure 9. Median total sciaenid densities (fish/ 100m ³) captured at surface depths (red) and non-surface (ns) depths (blue).	36

Figure 10. Median sciaenid densities (fish/ 100m³) captured at surface depths (red) and non-surface depths (blue) for samples collected during the Day with data restricted to fall months (September, October, and November). 37

Figure 11. Median total sciaenid densities (fish/ 100m³) captured at surface depths (red) and non-surface depths (blue) for samples collected during the night with data restricted to fall months (September, October, and November). 38

Figure 12. Scree plot of PCA of family densities. 83.5% of the variance in the data is explained by the first dimension..... 39

Figure 13. Loadings plot for principal component 1. 39

Figure 14. Loadings plot for principal component 2. 40

Figure 15. Loadings plot for principal component 3. 40

Figure 16. Loadings plot for principal component 4. 41

Figure 17. PCA biplot for PC1 and PC2..... 41

Figure 18. PCA biplot for PC3 and PC4..... 42

Figure 19. PCA biplot for PC1 and PC2..... 42

Figure 20. PCA biplot for PC3 and PC4..... 43

Figure 21. PCA biplot for PC1 and PC2. Points are colored by photoperiod (day and night) and loading vectors indicate an increase in family density. 43

Figure 22. PCA biplot for PC3 and PC4. Points are colored by photoperiod (day and night) and loading vectors indicate an increase in family density. 44

Figure 23. PCA biplot for PC1 and PC2. Points are colored by depth stratum (surface and non-surface) and loading vectors indicate an increase in family density..... 44

Figure 24. PCA biplot for PC3 and PC4..... 45

LIST OF TABLES

	Page
Table 1. Larval density (fish/100m ³) of families arranged by sampling month resulting in total averaged (mean ± standard deviation).....	22
Table 2. Larval density (fish/100m ³) of families arranged by sampling time (day or night) resulting in total averaged (mean ± standard deviation).....	23
Table 3. Larval density (fish/100m ³) of families arranged by tidal cycle (ingoing or outgoing) resulting in total averaged (mean ± standard deviation).....	24
Table 4. Larval density (fish/100m ³) of families arranged by sampling depth (surface tow or not surface tow) resulting in total averaged (mean ± standard deviation).....	25
Table 5. Sciaenid species density (fish/100m ³) arranged by sampling month resulting in total averaged (mean ± standard deviation).....	26
Table 6. Sciaenid species density (fish/100m ³) arranged by sampling time (day or night) resulting in total averaged (mean ± standard deviation).....	27
Table 7. Sciaenid species density (fish/100m ³) arranged by sampling depth (surface or not surface) resulting in total averaged (mean ± standard deviation).....	27
Table 8. Sciaenid species density (fish/100m ³) arranged by sampling tidal cycle (ingoing or outgoing) resulting in total averaged (mean ± standard deviation).	28
Table 9. Morphological identification vs. genetic identification of paralichthyids from February sampling.....	29
Table 10 . ANOVA model results for total larval density vs the factors month, time of day, depth of net, and tidal cycle.....	31

Table 11. ANOVA model results for total larval density collected during the day vs the factors month, depth of net, and tidal cycle.	32
Table 12. ANOVA model results for total larval density collected during the day grouped by month vs the factors of tidal cycle.	32
Table 13. ANOVA model results for total larval density collected during the night vs the factors month, depth of net, and tidal cycle.	33
Table 14. ANOVA model results for total larval density collected during the night grouped by month vs the factors of net depth.	34
Table 15. ANOVA model results for Sciaenid larval density vs the factors month, time of day, depth of net, and tidal cycle.	36
Table 16. ANOVA model results for sciaenid larval density collected during the day vs the factors depth of net and tidal cycle.	37
Table 17. ANOVA model results for sciaenid larval density collected during the night vs the factors depth of net and tidal cycle.	37

1. INTRODUCTION

Estuaries, coastal bays, and lagoons, provide important nursery habitat for juvenile fishes and shellfish. This essential habitat is structurally complex and provides protection from predators and increases foraging opportunities for juvenile fish, both of which increase the chance of survivorship (Minello, 1999). Inlets are a prominent feature of many coastal waterways that connect the ocean to protected inshore habitat and are dynamic environments with distinct seasonal changes in environmental parameters, such as water temperature, percent oxygen saturation, and salinity. Larval stages of many fish and shellfish species must pass through inlets, which act as a bottleneck for the transport of larvae from oceanic spawning grounds to nursery habitat (Boehlert & Mundy, 1988; Schieler et al., 2014). Anthropogenic factors such as increased turbidity from boating activity and artificial light can disorient larvae, can reduce the rate of successful ingress into bays and estuaries (Collin & Hart, 2015). It is vital to understand what drives patterns of ichthyoplankton ingress which can be done by understanding 1) the composition of ichthyoplankton 2) the shifts in composition over time and 3) what environmental factors correspond with shifts in composition. All three components help us to understand the details larval ingress and thus allowing us to mitigate the human activities that might negatively impact ingress.

In Texas, coastal recreational sportfishing accounts for \$1.79 billion each year, with the majority of funds being attributed to red drum fishing (Southwick, 2006). While some species spend their entire life history in estuaries such as many species of gobiids, this research will focus on estuarine-dependent, marine species that use estuaries as nursery grounds during their early life stages. These obligate estuarine-dependent marine fishes are species that require an estuary for part of their life cycle and can either spawn in the estuary and move offshore as they

age, or spawn offshore and move into the estuary during their larval stage (Able, 2005). In fact, 95% of the commercial fishing harvest in the Gulf of Mexico (GOM) is attributed to estuarine dependent species (Baccus, 1999). Because this research focuses on movement of larvae through inlets, the fish species which spawn offshore in the Gulf of Mexico (GOM) and move into estuaries for nursery habitat will be the primary focus. Since ichthyoplankton have limited horizontal swimming capabilities against strong currents, which often occur in coastal inlets, they are thought to rely heavily on environmental cues and position in the water column for transport in and out of the protected waters. Major cues that can affect ingress include seasonal temperature change, tidal variation, and daylight duration (Wiseman Jr. & Dinnel, 1988). There are two primary mechanisms of larval transport through inlets: one being passive and the other being active transport.

1.1. Passive Transport of Larval Planktonic Organisms

Passive transport models view planktonic larvae as passive particles which are solely moved by physical forces. Some studies use 2 or 3-dimension models in which the planktonic larvae do not respond to any environmental cues and are akin to passive particles like grains of sand or pieces of plastic (Pietrafesa & Janowitz, 1988; Seabergh, 1988; Wang, 1988). These models are heavily driven by three components: wind, tidal fluxes, and physical geography of the estuarian inlet, with the current velocity and overall water flow being modeled. Tidal flow creates a plume of estuarine water in the marine environment during the ebb tide and a plume of ocean water in the estuary during the flood tide. Passive transport studies characterize tidal plumes as the major transport mechanism into and out of estuaries (Pietrafesa & Janowitz, 1988; Seabergh, 1988; Wang, 1988). The tidal changes and transport currents can also be affected by wind velocity, which is often a key factor in estuaries in the eastern GOM (Brown et al., 2005).

While modeling larvae as passive particles provides a good basis for understanding complex physical transport through coastal inlets, it is seen as an incomplete representation by many in the scientific community today (Whitefield et al., 2023).

1.2. Active Transport of Larval Planktonic Organisms

Active transport models view planktonic larvae not as passive particles but as active individuals, responding to cues in the environment. More recent studies, such as Faillettaz et al. (2018), have found that including simple swimming behavior in dispersion models increases accuracy as compared to passive larval models. Many studies have shown evidence of behavioral responses to environmental cues involved in current fluctuations (Boehlert & Mundy, 1988; Baptista et al., 2020). Vertical migration is known to occur in planktonic species with plankton moving up in the water column at night and down during the day to avoid predators and/or harsh UV rays, or to seek food items. There is some evidence that ichthyoplankton use vertical movement to facilitate transport through inlets (Schieler et al., 2014; Whitfield et al., 2023; Wenner, 2005). In their review, Boehlert & Mundy (1988) found that the use of vertical movements to facilitate transport through inlets was highly variable among species (Figure 1). *Paralichthys* spp. in North Carolina were found in higher concentration on flood tides during the night as compared to ebb tide during the day, leading Weinstein et al. (1980) to speculate that post-larval flounder shifted to the bottom during ebb tides (Figure 1). By comparison, Weinstein et al. (1980) found that Atlantic croaker, (*Micropogonias undulatus*), remained deeper in the water column both day and night (Figure 1). The phenomenon noted by Weinstein et al. (1980) is commonly known as selective tidal stream transport (STST), in which organisms use tidal cycles, ebb or flood, for transportation into and out of estuaries (Gibson & Atkinson, 2001). While the type of tidal transportation is known to vary across species, season, ontogeny, and

other environmental factors; ichthyoplankton that spawn offshore generally exhibit flood tide transportation during the night. Flood tide transportation is characterized by individuals moving upwards in the water column during flood tide to move up estuaries to nursery grounds and sinking deeper into bottom waters to remain in estuaries (Gibson & Atkinson, 2001). Boehlert & Mundy (1980) asserted clear evidence for behavioral responses to tidal forces but what cues these responses is less clear. Even though there is strong evidence of a diel component to STST, there are also other transportation cues such as salinity (Gibson & Atkinson, 2001). In another study, Téodosio et al. (2016) present the Sense Acuity and Behavioral (SAAB) hypothesis which states that ichthyoplankton use a hierarchy of cues including odor, sound, visual, and geomagnetic. The SAAB hypothesis has two components, offshore and nearshore, and is based on studies of post-flexion larvae across multiple temperate species. When larvae are offshore, the SAAB hypothesis maintains that they use cues from sensory organs that detect the sun's intensity and position and earth's geomagnetic field. Nearshore, larvae will exhibit behaviors in response to estuarine cues such as odor, sound, and visual cues. Baptista et al. (2020), found that both post and pre-flexion white seabream (*Diplodus sargus*) larvae can swim at speeds greater than most ocean currents, showing that these larvae are not restricted to passive dispersal. Salinity cues have been most apparent in shrimp and crab species (Boehlert & Mundy, 1980), which have been shown to recruit into estuarine habitat as juveniles more successfully in years with high rainfall (Boehlert & Mundy, 1980).

Salinity cues are particularly important for this research because as human water usage increases while freshwater stores decrease, desalination plants and their effluents will apply more pressure to coastal ecosystems. The salinity will increase wherever the briny discharge of a desalination plant is located within an estuary, which can be further exacerbated by slow flushing

times and bottom topography. The high levels of salinity may not only cause osmotic stress on the organisms but may interfere with inlet transport cues.

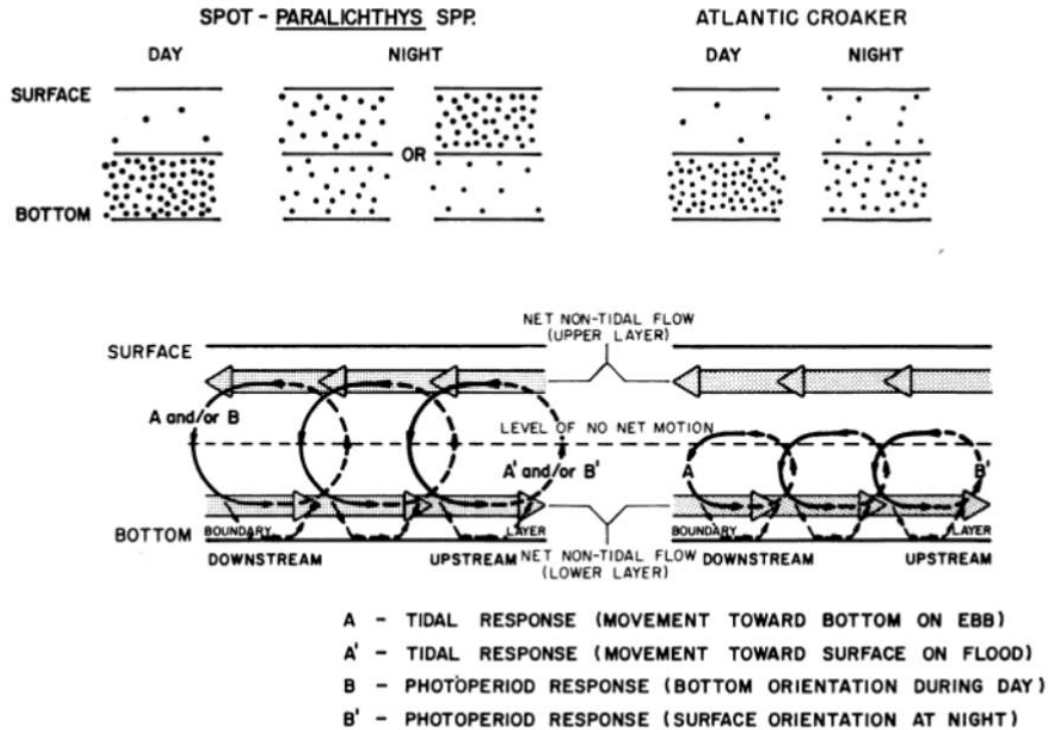


Figure 1 - Conceptual model displaying the response of three taxa (*Leiostomus xanthurus*, *Micropogonias undulatus*, and *Paralichthys* spp.) of ichthyoplankton to photoperiod and tidal flow. Taken from Weinstein et al. 1980.

1.3. Larval Transport through the Aransas Pass Inlet System

The Aransas Pass Inlet system connects the GOM waters with several bays: Aransas Bay, Corpus Christi Bay, Nueces Bay, Redfish Bay, Copano Bay, and St Charles Bay. The nearest inlet is 35 km north and 125 km south of the Aransas Pass Inlet (Pass Cavallo and Mansfield Pass respectively), thus making the Aransas Pass Inlet an important bottle neck for ichthyoplankton seeking nursery habitat. Even though larval stages are crucial in the life history of many marine species, only a few studies have been conducted in the geographic area, with knowledge of the vertical distribution of larvae in the water column being scarce. In shallow coastal estuaries such as Aransas Bay and Corpus Christi Bay, wind and tidal forcing are the two

key physical components (Brown et al., 2005). Brown et al.'s (2005) 2-dimensional model has a very accurate at predicting pulses of larval recruitment, using only physical passive transport data. When models with and without wind forcing were compared, wind forcing could at least partially account for increases in particles into the bay (Brown et al., 2005). However, that study simplified the bay system and lacked the complex bathymetry required. In another study, Holt & Holt (2000) found that during the day concentration of larvae was higher in bottom tows, while at night the number of larvae was consistent throughout the water column, indicating a relationship between photoperiod and depth. The differing densities of ichthyoplankton at varying depths supports the SAAB hypothesis. The conclusion of these studies is somewhat limited, however, because they focused on only two species, red drum (*Sciaenops ocellatus*) and spotted seatrout (*Cynoscion nebulosus*) and were limited to Lydia Ann Channel and a six-week period of sampling in late summer/early fall (Holt & Holt, 2000). A more recent and comprehensive study of blue crab larvae (megalops) showed the highest amount of blue crab megalops in their GOM and Aransas Pass Inlet sampling sites during the months of October and February (Weatherall et al., 2018). However, this study was focused on only settlement stage larvae gathered with an artificial substrate collector, which only gives insight into one life-history stage. Information about other commercially important species is lacking in Aransas Bay and few studies implement year-round sampling.

1.4. Potential effects of desalination brine plume on larval health & survival

In recent years, desalination plants have become a sought-after source of drinking water in the United States (Rao et al., 2018). While increasing access to a much-needed resource, desalination plants can have harmful effects on coastal marine environments. Desalination plants intake seawater, through various methods, remove the salt, and discharge brine back into the

coastal environment. Both the intake of seawater and discharge of brine by desalination plants can be detrimental to marine fauna (Missimer & Maliva, 2018; Miri & Chouikhi, 2005; Petersen et al., 2018). Intake systems can cause impingement, entrainment, and subsequent removal, of smaller marine organisms, particularly larvae and eggs. The mitigation of intake velocity and implementation of protective mesh screen coverings for intake heads has been shown to reduce the effects of impingement (Missimer & Maliva, 2018; Petersen et al., 2018). The discharge of brine is perhaps more harmful because brine not only increases the surrounding salinity but can change water temperature and may contain harmful antifouling chemicals (Miri & Chouikhi, 2005). An increase in temperature and salinity is associated with lower oxygen solubility in water, increased physiological stress on fishes, and increased turbidity of seawater (Miri & Chouikhi, 2005). Abrupt changes in salinity have been known to affect species growth differently, with an increase in salinity slowing growth rate in *Micropogonias undulatus* (Peterson et al., 1999) and increasing growth rate in *Paralichthys lethostigma* (Moustakas et al., 2004). Turbidity can create both positive and negative conditions for ichthyoplankton; increasing the ability to hide from predation (Fisken et al., 2002; Carreon-Martinez et al., 2014) but decreasing their ability to detect prey (Salonen et al., 2009). Anti-fouling chemicals increase toxicity and are known to impact the embryonic development of fishes (Petersen et al., 2018) and cause increased physiological stress. These factors can not only harm individual larva, but they can also be detrimental to their food sources, reducing the amount of zooplankton available and thus reducing the chances of feeding success for larval fishes. The growth-survival paradigm, first introduced by Anderson (1988), suggests that slower growing individuals have a reduced chance of survival because they remain in the larval stage longer and are thus more susceptible to starvation and predation (Pepin et al., 2014). There are several proposed desalination plants in

the coastal Texas area, including a proposed desalination plant on Harbor Island in Port Aransas, TX which is near the geographic focus of this study (Figure 2). Unfortunately, few published studies have assessed the potential impacts of these plants on subtropical waters seen in coastal Texas.

1.5. Objectives and Hypothesis

The objectives of this study were:

- 1) To identify patterns of larval transport through the Port Aransas Inlet (TX) for different fish families and species during the months of June, July, September, October, November, and February, including vertical position in the water column using depth stratified sampling techniques.
- 2) Investigate factors influencing larval transport in the Port Aransas Channel system, as example for an inlet into mixed estuaries, including tide, time of day, and time of year.

Null Hypothesis: None of the factors (tide, time of day, month, and net depth) will be significant predictors of larval density.

Alternative Hypothesis: Some or all factors (tide, time of day, month, and net depth) will be significant predictors of larval density.

2. MATERIALS & METHODS

2.1. Study Site

Three channels comprise the Aransas Pass Inlet System: Lydia Ann Channel, Aransas Pass Channel, and Corpus Christi Ship Channel. The largest, Corpus Christi Shipping Channel, is approximately 13.7 meters deep by 121.9 meters wide and acts as the main pathway for large cargo and tanker vessels traveling to the Port of Corpus Christi. There are ongoing plans to increase the size of the Corpus Christi Shipping Channel to 16.5 meters deep and 161.5 meters wide (Torres, 2020). The Aransas Pass Channel is approximately 14.3 meters deep and 40 meters wide, with proposals for dredging and extending the channel into the Gulf of Mexico (Brown et al., 2005; Parker, 2018). Lydia Ann Channel is approximately 7.6 meters deep and 250 meters wide at the entrance narrowing to 4 meters deep and 40 meters wide near the exit to Aransas Bay (Brown et al., 2005). The Corpus Christi Shipping Channel, accounts for 60% of the water flow from the Gulf of Mexico (Brown et al., 2005) into the Aransas Bay System. The tides in the area are diurnal to mixed diurnal-semidiurnal (Brown et al., 2005) and are highly wind driven. The bottom of all three channels mainly consists of sand and silt, with seagrass beds compromising 11% of the bottom of the surrounding bays and the majority of seagrass occurring in Redfish Bay (Brown et al., 2005).

2.2. Sampling Design

To assess ichthyoplanktonic composition/density, sampling site was located in each channel (Aransas Pass Inlet, AP1; Corpus Christi Shipping Channel, CC1; and Lydia Ann Channel, LA1; Figure 2) with a fourth being located in between the jetties of the Inlet itself (Port Aransas Channel; PA1 located on Figure 2). Sampling occurred over the course of several

months starting in June of 2021 and ending in February of 2022 to account for seasonal differences in spawning activity among fishes.

Both ingoing and outgoing tides were sampled for a comparative analysis of passive and active transport of the plankton. Samples were also collected during daylight and nighttime hours, as previous studies have shown the importance of diurnal vertical movement (Holt & Holt 2000). Lastly, 2-3 discrete depths were sampled (depending on the average depth of the channel; 3 depths for CC1 & PA1 and 2 depths for AP1 & LA1) because ichthyoplankton are known to move horizontally in the water column depending on photoperiod and tide. The Pythagorean theorem was used to calculate the amount of tow line needed for the desired depth of sampling as described in the NOAA SEAMAP Operations Manual. An ideal angle of 45° was used in the equation along with total depth and desired depth. The tow line was marked in one- and five-meter increments and quickly lowered to desired depth using a winch system. The line angle was continually measured during the tow to ensure stability around 45° . A total of 13 sampling days were completed with every combination of site, photoperiod, tidal phase, and depth strata occurring, with exceptions due to poor weather conditions or high levels of marine traffic.

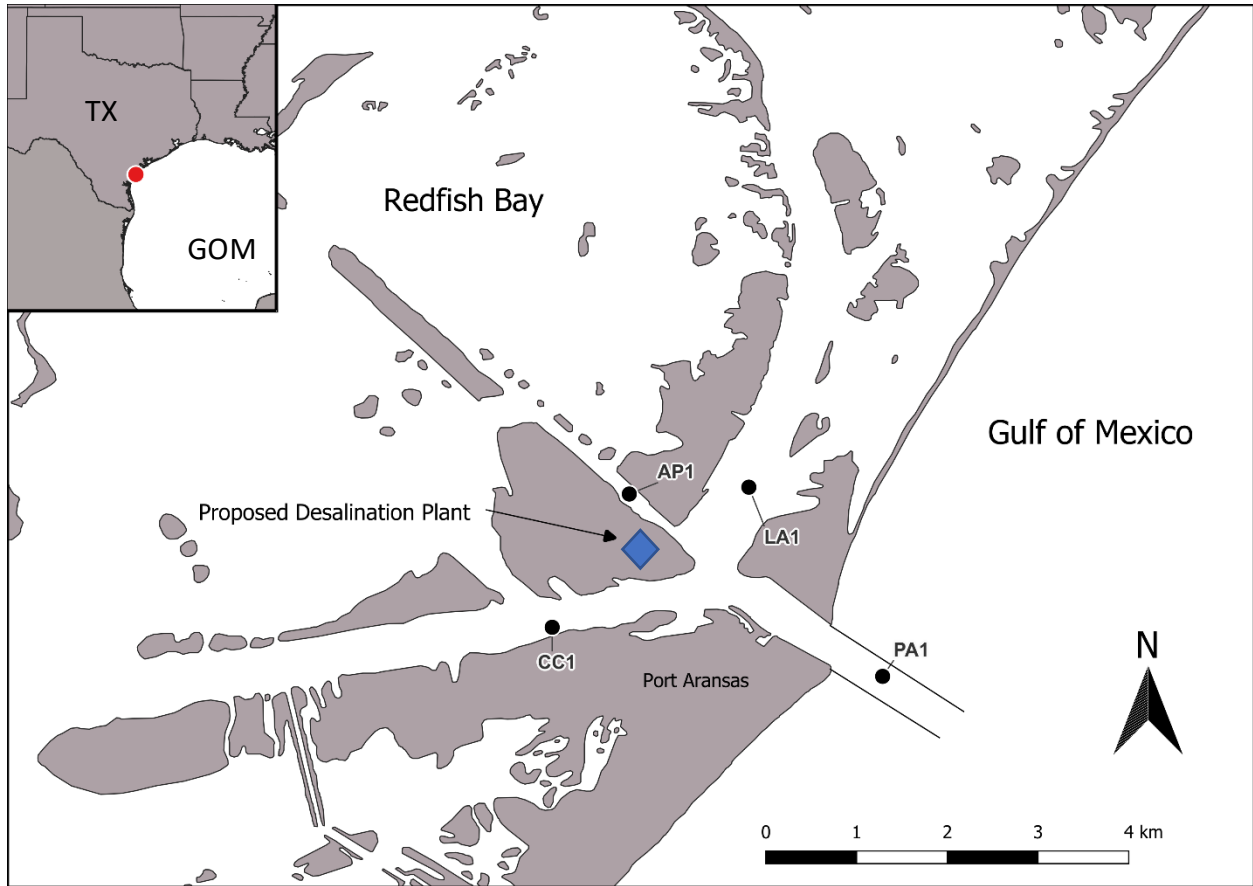


Figure 2 - Map of sampling area in coastal Texas displaying sampling sites Corpus Christi Channel, Aransas Pass Channel, Lydia Ann Channel, and Port Aransas (CC1, AP1, LA1, & PA1 respectively). The blue diamond indicates the location of the proposed desalination plant.

2.3. Water Quality Measurements

During each sampling day and at every station, temperature, salinity, pH, and O₂ concentration profiles were taken using a multiparameter sonde (YSI exo1 or YSI V2). These measurements were collected once per photoperiod and tidal change, by slowly lowering the device through the water column. A sampling event consisted of samples taken for ingoing and outgoing tide once during night hours and once during daylight hours. NOAA buoy RTAT2 water quality measurements were taken for the sampling done in September due to equipment difficulties.

2.4. Plankton Sample Collection & Processing

Each sample was collected using a ring net (75 cm diameter, 500 μm mesh width, 5:1 diameter length ratio) equipped with a mechanical flow meter (General Oceanics). The initial tow occurred just below the surface, the second mid water column, and the final tow just above the seafloor (all depending on total depth of the station). The net was towed for 3-10 minutes, depending on time of day (photoperiod), at 1-2 knots for a goal of 100 m^3 of water volume sampled per net tow. All samples were initially preserved in a 50% ethanol solution, then filtered and stored in 100% ethanol within 24 hours of collection. For processing in the lab, plankton samples were split if necessary, with a Folsom Plankton Splitter (total of two subsamples) and subsamples were used to quantify larvae. All ichthyoplankton were identified to the family level, with sciaenids identified to genus and species when possible. Larger individuals in the genus *Menticirrhus* were identified to species but smaller individuals were combined into one group due to the difficulty of accurately differentiating among *Menticirrhus americanus* (southern kingfish), *M. littoralis* (Gulf kingfish), and *M. saxatilis* (northern kingfish). For species of particular importance where larvae were hard to identify, DNA Barcoding was used to verify identifications based on morphology. Paralichthyids were identified to genus and species using DNA barcoding because they are difficult to reliably identify using morphological characteristics. The following species were identified in the barcoding of paralichthyids: *Paralichthys lethostigma* (southern flounder), *Paralichthys albigutta* (Gulf flounder), and *Citharichthys spilopterus* (bay whiff). All individuals classified as unknown were considered in too poor condition to be accurately identified by morphological characteristics. Larval density was calculated using the following equation for the water volume:

$$\text{Filtered water volume} = \pi \times r^2 \times \frac{(\text{Flowmeter final} - \text{flowmeter initial}) \times 26873}{999,999}$$

with r = the radius of the net opening and 26873 = rotor constant for the flowmeter (General Oceanics Inc, 2018).

2.5. Ichthyoplankton Community Analysis

2.5.1. Total Density

Total larval density of each sample was calculated with the following equation:

$$\text{Total larval density (fish per } 100\text{m}^3) = \frac{\text{fish count}}{\text{filtered water volume}} \times 100$$

All analysis was completed in R and R Studio using the *gls* (generalized least squares) function in the package *nlme* v4.1.1 (Hankin, 2006; Pinheiro et al., 2021; R Core Team, 2021; RStudio Team, 2015). A full model with 2-way interactions included was used to compare total larval density for each sample with time of day, tide, net depth, and month. The factor, season, was removed because it repeated the factor of month and 3-way interactions were not included because they are extremely complex and would result in little interpretable results. The sampling completed in June and July was removed from this analysis because outgoing tide was not sampled during those dates. An analysis of the distribution of larval density across all samples showed that the residuals were non-normally distributed with a biological wall at 0 fish/100m³ and a long upper tail. To account for this, total larval density was log transformed using the natural log. Generalized least squares estimation method was chosen because it is best suited for continuous variables and can be used to compare interactions among factors.

2.6. Ichthyoplankton Transport Comparisons

2.6.1. Family Level Diversity

Family level diversity analysis was completed with the same methods as the analysis for the total larval density. The families Sciaenidae and Paralichthyidae were chosen based on their economic importance and their spawning migratory behavior. Only Fall, the peak spawning

season, was analyzed for the Sciaenidae to reduce the amount of zero values (ties) and to focus on spawning time. The residuals of the larval density data for sciaenids were not normal even after log transforming the data, so the ANOVA results were verified using a Wilcoxon rank sum exact test.

2.6.2. PCA

Principal component analysis (PCA) was conducted to explore the correlation between the ichthyoplankton community (family level) and tide, depth, photoperiod, and month. Analysis was performed in R and R Studio using the *prcomp* function. Scree plots were created using *factoextra* v1.0.7 (Kassambara & Mundt, 2020). The first, second, third, and fourth principal component axes were used to assess community composition as they accounted for a sum of 99.6% of the variation (Figure 13). Four families (Sciaenidae, Gobiidae, Clupeidae, and Sparidae) which accounted for the highest correlation to each principal component were the focus of the analysis.

2.6.3. Sciaenid Species Density

Over 93% of the individual sciaenids collected were identified as *Micropogonias undulatus*, which left little data for complete analysis of each sciaenid species. Thus, sciaenid species density was not individually analyzed and *Sciaenidae* family analysis was understood to be driven by *M. undulatus*.

2.6.4. Paralichthyidae Family

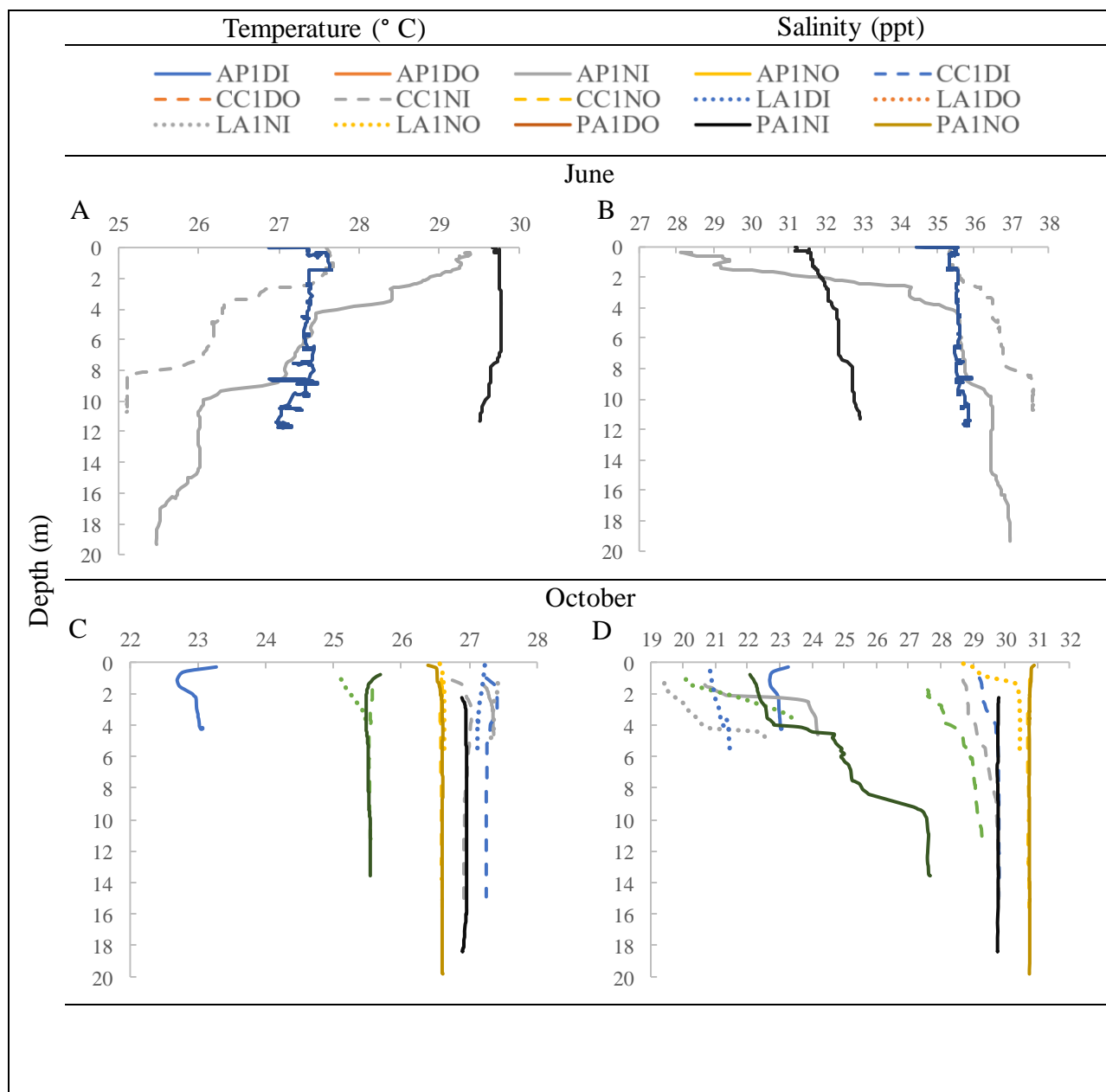
Because the majority of paralichthyids identified in the samples were *Citharichthys spilopterus* (bay whiff), which spend their life cycle in bays and estuaries, the paralichthyids were not analyzed on a family level. This study's aim was to explore the differences in larval densities of species whose adults migrate offshore to spawn and whose larvae are transported

into the bays and estuaries for nursery habitat. Furthermore, barcoding showed that morphological IDs to species were not always accurate, so the author did not feel comfortable with further analysis until barcoding could be completed for all individuals.

3. RESULTS

3.1. Water Quality

Across all samples pH ranged 7.5 to 8.4 and did not vary in the water column with depth. Both the highest and lowest pH levels were found at station LA1. June had the highest salinities warmest temperatures (Figure 3). The coolest temperatures were measured in February and the lowest salinities were recorded in October (Figure 3).



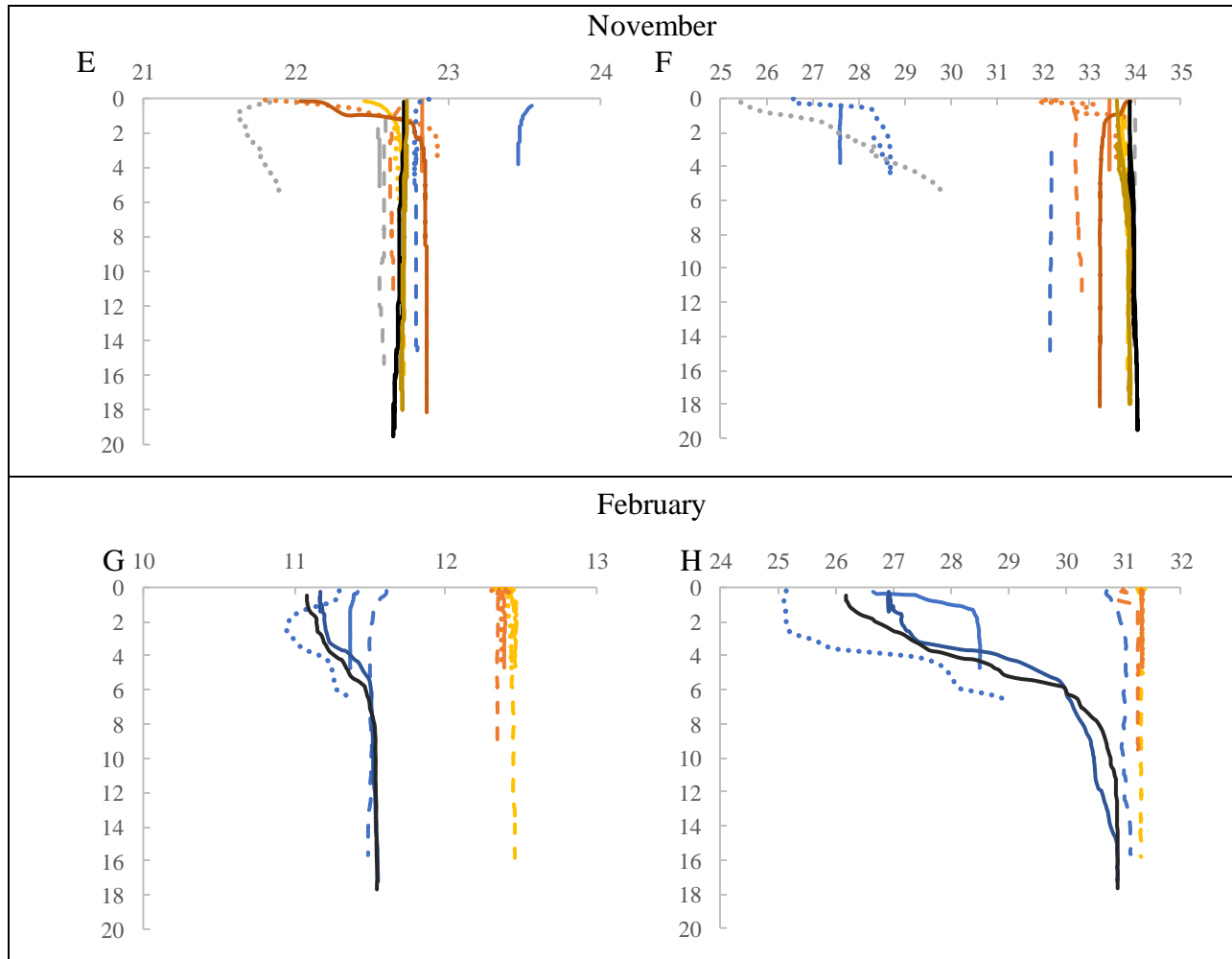


Figure 3 - Depth profiles of temperature ($^{\circ}$ C) on the left-hand side and salinity on the right-hand side arranged by sampling month. Profiles were taken for stations Corpus Christi (CC1), Aransas Pass (AP1), Lydia Ann (LA1), and Port Aransas (PA1) during day (D) and night (N) for ingoing (I) and outgoing (O) tides. June represented by A and B, October by C and D, November by E and F, and February by G and H.

3.1.1. June & July

Water quality data was collected in June only, and not collected in July, because the sampling for June and July was considered one sampling session. The average temperature in June ranged from 25 to 30 $^{\circ}$ C. Stations AP1NI and CC1NI both showed stratification between warmer surface waters and cooler waters as depth increased.

Salinity ranged from 28 to 38 with highest salinity measured in June and July. Similarly, to temperature, stations AP1NI and CC1NI were stratified with lower salinity at the surface and increasing salinity with depth.

Dissolved oxygen (DO) concentrations were consistent throughout the water column for stations PA1DI and PA1NI, approximately 5.5 mg/L and 4 mg/L respectively. Stations AP1NI and CC1NI showed stratification with higher DO concentrations at the surface, 5-6 mg/L, and decreasing concentration with an increase in depth.

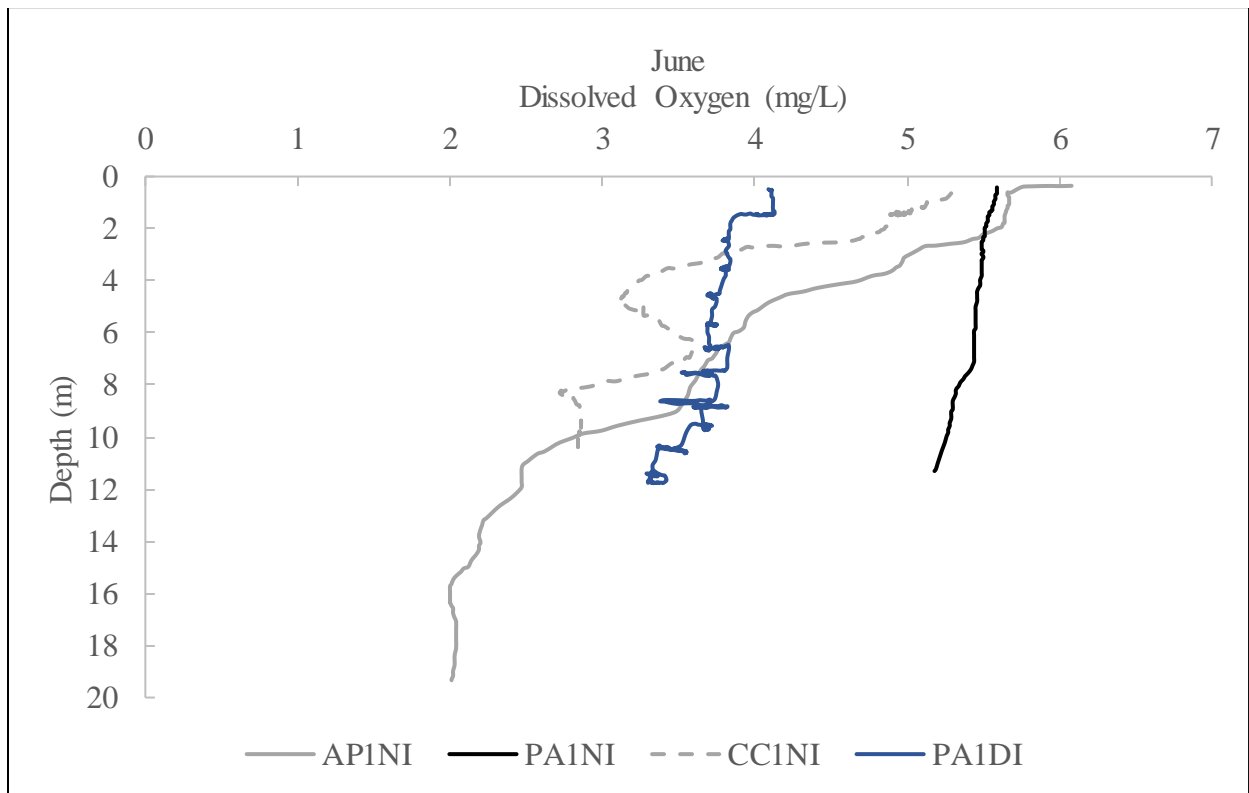


Figure 4 - Depth profile of dissolved oxygen (DO) concentrations (mg/L) for sampling stations Corpus Christi night in (CC1NI), Aransas Pass night in (AP1NI), Port Aransas night in (PA1NI), and Port Aransas day in (PA1DOI) taken during June.

3.1.2. October

The average temperature in October ranged from 25 to 28 °C depending on station, with complete mixing of the water column (Figure 3 C). Figure 3 D displays the average salinity for

the month of October, with a few instances in which the water column showed slight stratification but otherwise was well mixed. The stations with slight stratification had a surface layer of water with lower salinities, on average 22, and an increasing salinity measurement with depth. The stations with slightly stratified waters include PA1DO (slack), LA1NO (slack), LA1NI, LA1DO, CC1NI (slack), CC1DO, CCDI, and AP1NI (slack).

Dissolved oxygen concentrations for the month of October ranged from 6 to 8 mg/L throughout the water columns for all stations.

3.1.3. November

November water temperatures ranged from 22 to 24 °C (Figure 3 E) and showed consistent mixing across all stations. Most stations in November showed consistent salinities as well with an approximate salinity 34, (Figure 3 F). Salinity was stratified in only one station, LA1, for three of the samples, LA1DI (slack), LA1DO, and LA1NI, this month seen in Figure 3 F. Dissolved oxygen concentrations ranged from 6.5 to 7.7 mg/L for all stations and remained mixed within stations.

3.1.4. February

During February water temperatures ranged from 11 to 13 °C with complete vertical mixing for all stations (Figure 3 G). Salinity for most stations was vertically mixed ranging from 31 to 32 (Figure 3 H). The water column was slightly stratified for stations LA1DI, AP1DI, PADI, and PA1NI, seen in salinity profiles (Figure 3 H). Dissolved oxygen concentrations for February ranged from 9 to 10 mg/L for all stations and were mixed within stations.

3.1.5. September

For Corpus Christi Channel at the approximate location of CC1, water temperature ranged 30 to 31 °C at the surface waters, (Figure 5). This buoy is located on the southern edge of

the channel unlike CC1 which was center of the channel and only has data from the surface waters, not a complete profile. Salinity, pH, and oxygen concentration data for this month were unavailable.

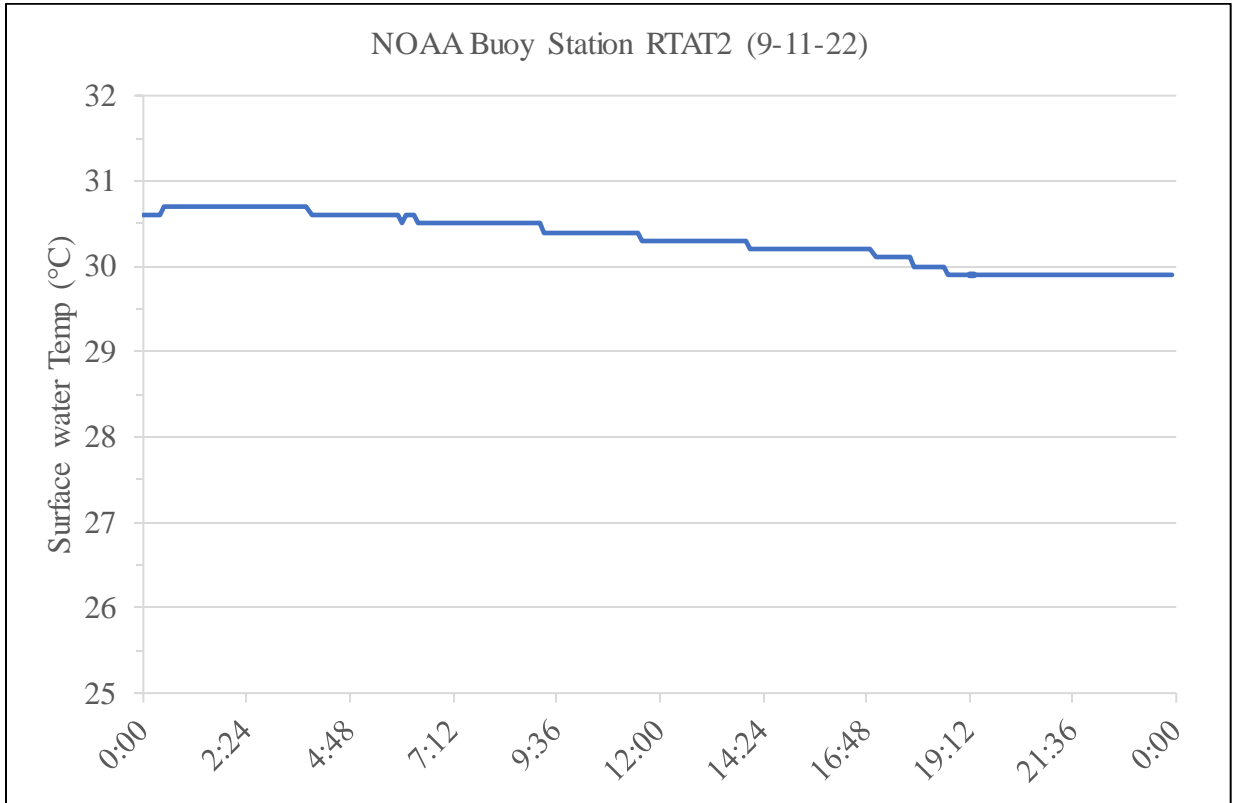


Figure 5 - Data provided by NOAA (bouy station RTAT2) of surface water temperatures in the Corpus Christi Channel for the sample date of September 11th, 2022.

3.2. Community Composition

A total of 150 net tows were completed over the course of 11 days and across six months: June, July, September, October, November, and February. Over the course of the study 18,076 ichthyoplankton were collected, and total larval densities ranged from 0 to 1142 Ind./100m³ in individual net hauls.

3.2.1. Family Composition

A total of 17,645 fish were identified to one of 22 families and an additional 400 individuals could not be identified to family but were identified as the ordinal level (Tables 1-4).

Thirty-one individual larvae were not identified due to poor condition. Numerically dominant families for every sampling month included Sciaenidae, Clupeidae, and Gobiidae. The most abundant families differed based on, month, time of day, tidal cycle, and net depth. In the month of September, engraulids (6 fish/100m²) were abundant and had similar concentrations as clupeids (7 fish/100m²; Table 1). Sciaenids were most abundant in October and November, with concentrations up to five times greater than the concentrations of other families (Table 1). In February there was a decrease in the concentration of sciaenids, with sparids and clupeids being the most abundant (Table 1). During the day sparids and clupeids were the most abundant families, while during the night sciaenids and gobiids were the most abundant (Table 2). Sciaenids, gobiids, and clupeids were consistently abundant across tidal cycles, while sparids were noticeably more abundant during the outgoing tide (Table 3). Sparids were also more abundant at non-surface depths than at surface depths (Table 4).

Table 1 - Larval density (fish/100m³) of families arranged by sampling month resulting in total averaged (mean ± standard deviation). Dash (-) denotes no taxa collected in tow.

Family	Month Larval Density (fish/100m ³)					Total Averaged (mean ± SD)
	June & July '21	September '21	October '21	November '21	February '22	
Archiridae	0.30	-	-	-	-	0.06 ± 0.37
Atherinopsidae	-	-	-	-	0.07	0.02 ± 0.12
Blennidae	0.34	0.51	0.32	-	-	0.22 ± 0.59
Carangidae	0.70	0.12	1.80	0.48	-	0.65 ± 1.81
Clupeidae	3.16	6.74	40.25	11.23	21.38	19.15 ± 33.94
Clupeiformes	8.36	2.50	4.13	0.83	0.03	2.51 ± 8.73
Cynoglossidae	0.39	0.25	0.51	0.29	-	0.30 ± 1.23
Engraulidae	1.97	5.91	2.61	1.52	-	2.05 ± 4.93
Gerreidae	3.40	0.38	0.06	0.20	-	0.77 ± 5.63
Gobiidae	10.68	36.35	18.50	10.54	2.67	14.71 ± 45.70
Hemiramphidae	0.25	0.08	-	-	-	0.06 ± 0.45
Lutjanidae	0.05	-	-	-	-	0.01 ± 0.08
Microdesmidae	0.17	-	-	-	-	0.02 ± 0.19
Mugilidae	-	-	-	-	0.19	0.04 ± 0.43
Ophichthidae	-	-	-	0.52	1.66	0.51 ± 2.07
Ophidiidae	-	-	0.15	0.06	0.07	0.07 ± 0.26
Paralichthyidae	0.26	0.67	0.91	2.18	4.18	1.85 ± 5.95
Sciaenidae	2.55	2.00	108.02	98.29	6.99	51.41 ± 138.77
Sparidae	0.08	-	-	0.01	22.64	5.32 ± 29.32
Stromateidae	-	-	0.03	0.01	-	0.01 ± 0.08
Syngnathidae	0.31	0.17	0.12	0.23	-	0.14 ± 0.45
Triglidae	-	-	0.08	-	-	0.02 ± 0.15
Unknown	10.28	0.08	0.05	0.09	0.02	1.10 ± 11.37
Total	43.23	55.76	177.54	126.49	59.88	100.99

Table 2 - Larval density (fish/100m³) of families arranged by sampling time (day or night) resulting in total averaged (mean \pm standard deviation). Dash (-) denotes no taxa collected in tow.

Family	Time of Day Density (fish/100m ³)			Total Averaged (mean \pm SD)	
	Day	Night			
Archiridae	0.03	0.08	0.06	\pm	0.37
Atherinopsidae	-	0.03	0.02	\pm	0.12
Blennidae	0.31	0.13	0.22	\pm	0.59
Carangidae	0.36	0.92	0.65	\pm	1.81
Clupeidae	2.90	33.91	19.15	\pm	33.94
Clupeiformes	0.46	4.37	2.51	\pm	8.73
Cynoglossidae	0.01	0.57	0.30	\pm	1.23
Engraulidae	0.45	3.51	2.05	\pm	4.93
Gerreidae	0.06	1.42	0.77	\pm	5.63
Gobiidae	0.89	27.27	14.71	\pm	45.70
Hemiramphidae	0.10	0.02	0.06	\pm	0.45
Lutjanidae	-	0.02	0.01	\pm	0.08
Microdesmidae	-	0.03	0.02	\pm	0.19
Mugilidae	-	0.08	0.04	\pm	0.43
Ophichthidae	0.23	0.76	0.51	\pm	2.07
Ophidiidae	-	0.13	0.07	\pm	0.26
Paralichthyidae	0.40	3.17	1.85	\pm	5.95
Sciaenidae	1.36	96.85	51.41	\pm	138.77
Sparidae	3.41	7.05	5.32	\pm	29.32
Stromateidae	0.01	0.01	0.01	\pm	0.08
Syngnathidae	0.17	0.10	0.14	\pm	0.45
Triglidae	-	0.04	0.02	\pm	0.15
Unknown	0.06	2.04	1.10	\pm	11.37
Total	11.20	182.51			

Table 3 - Larval density (fish/100m³) of families arranged by tidal cycle (ingoing or outgoing) resulting in total averaged (mean \pm standard deviation). Dash (-) denotes no taxa collected in tow.

Family	Tide Larval Density (fish/100m ³)			Total Averaged (mean \pm SD)	
	in	out			
Archiridae	0.10	-	0.06	\pm	0.37
Atherinopsidae	0.01	0.03	0.02	\pm	0.12
Blennidae	0.23	0.21	0.22	\pm	0.59
Carangidae	0.66	0.64	0.65	\pm	1.81
Clupeidae	15.04	25.49	19.15	\pm	33.94
Clupeiformes	2.44	2.63	2.51	\pm	8.73
Cynoglossidae	0.45	0.08	0.30	\pm	1.23
Engraulidae	2.89	0.75	2.05	\pm	4.93
Gerreidae	1.24	0.05	0.77	\pm	5.63
Gobiidae	18.21	9.32	14.71	\pm	45.70
Hemiramphidae	0.10	-	0.06	\pm	0.45
Lutjanidae	0.02	-	0.01	\pm	0.08
Microdesmidae	0.03	-	0.02	\pm	0.19
Mugilidae	0.01	0.09	0.04	\pm	0.43
Ophichthidae	0.22	0.96	0.51	\pm	2.07
Ophidiidae	0.05	0.09	0.07	\pm	0.26
Paralichthyidae	1.36	2.60	1.85	\pm	5.95
Sciaenidae	56.60	43.40	51.41	\pm	138.77
Sparidae	0.93	12.09	5.32	\pm	29.32
Stromateidae	0.01	0.01	0.01	\pm	0.08
Syngnathidae	0.15	0.11	0.14	\pm	0.45
Triglidae	0.03	-	0.02	\pm	0.15
Unknown	1.77	0.05	1.10	\pm	11.37
Total	102.55	98.59			

Table 4 - Larval density (fish/100m³) of families arranged by sampling depth (surface tow or not surface tow) resulting in total averaged (mean \pm standard deviation). Dash (-) denotes no taxa collected in tow.

Family	Net Depth Larval Density (fish/100m ³)		
	surface	not surface	Total Averaged (mean \pm SD)
Archiridae	0.07	0.06	0.06 \pm 0.37
Atherinopsidae	0.04	0.01	0.02 \pm 0.12
Blennidae	0.22	0.23	0.22 \pm 0.59
Carangidae	0.59	0.70	0.65 \pm 1.81
Clupeidae	12.72	21.39	19.15 \pm 33.94
Clupeiformes	0.71	3.21	2.51 \pm 8.73
Cynoglossidae	0.02	0.39	0.30 \pm 1.23
Engraulidae	0.52	2.60	2.05 \pm 4.93
Gerreidae	1.35	0.59	0.77 \pm 5.63
Gobiidae	6.15	17.00	14.71 \pm 45.70
Hemiramphidae	0.07	0.06	0.06 \pm 0.45
Lutjanidae	-	0.01	0.01 \pm 0.08
Microdesmidae	-	0.02	0.02 \pm 0.19
Mugilidae	0.10	0.03	0.04 \pm 0.43
Ophichthidae	0.66	0.46	0.51 \pm 2.07
Ophidiidae	0.02	0.09	0.07 \pm 0.26
Paralichthyidae	1.67	1.96	1.85 \pm 5.95
Sciaenidae	22.93	64.28	51.41 \pm 138.77
Sparidae	10.41	3.66	5.32 \pm 29.32
Stromateidae	0.01	0.01	0.01 \pm 0.08
Syngnathidae	0.08	0.15	0.14 \pm 0.45
Triglidae	0.04	0.02	0.02 \pm 0.15
Unknown	2.21	0.77	1.10 \pm 11.37
Total	60.59	117.69	

3.2.2. Sciaenidae Species Composition

The majority of sciaenids were identified to species: *Cynoscion arenarius* (sand seatrout), *Cynoscion nebulosus* (spotted seatrout), *Cynoscion nothus* (silver seatrout), *Larimus fasciatus* (banded drum), *Menticirrhus americanus* (southern kingfish), *Micropogonias undulatus* (Atlantic croaker), *Sciaenops ocellatus* (red drum) (Table 5-8). For the months of October and November *M. undulatus* had the largest larval densities (Table 5). The densities for *M. undulatus* were approximately ten times greater than the densities for the next most abundant species, *S. ocellatus* in October and over two hundred times larger than *Menticirrhus* spp. in November (Table 5). *Micropogonias undulatus* had higher densities during night, non-surface depth, and ingoing tides (Tables 6-8). Although they did not display a large difference in density based on net depth, *S. ocellatus* had larger densities during night hours and outgoing tides (Tables 6-8).

Table 5 - Sciaenid species density (fish/100m³) arranged by sampling month resulting in total averaged (mean ± standard deviation). Dash (-) denotes no taxa collected in tow. Data is restricted to fall months: September, October, and November.

	Month Sciaenid Larval Density (fish/100m ³)				Total Averaged (mean ± SD)	
	September '21	October '21	November '21			
sciaenid spp.						
<i>Menticirrhus</i> spp.	0.14	1.70	0.44	0.76	±	1.29
<i>Cynoscion arenarius</i>	-	0.31	-	0.12	±	0.41
<i>Cynoscion nebulosus</i>	0.66	-	-	0.15	±	0.62
<i>Cynoscion nothus</i>	0.08	0.65	0.02	0.28	±	0.95
<i>Cynoscion</i> spp.	-	0.15	0.03	0.07	±	0.42
<i>Larimus fasciatus</i>	-	0.26	0.25	0.20	±	0.58
<i>Menticirrhus americanus</i>	-	0.21	0.08	0.11	±	0.50
<i>Micropogonias undulatus</i>	0.04	92.74	94.28	71.92	±	165.22
<i>Sciaenops ocellatus</i>	0.76	8.73	0.22	3.71	±	9.55
Unknown	0.17	3.19	0.07	1.33	±	7.62
Total	1.86	107.94	95.40			

Table 6 - Sciaenid species density (fish/100m³) arranged by sampling time (day or night) resulting in total averaged (mean ± standard deviation). Dash (-) denotes no taxa collected in tow. Data is restricted to fall months: September, October, and November.

sciaenid spp.	Fall Time of Day Sciaenid Larval Density (fish/100m ³)		
	Day	Night	Total Averaged (mean ± SD)
<i>Menticirrhus</i> spp.	0.07	1.61	0.84 ± 1.29
<i>Cynoscion arenarius</i>	-	0.24	0.12 ± 0.41
<i>Cynoscion nebulosus</i>	0.16	0.14	0.15 ± 0.62
<i>Cynoscion nothus</i>	0.04	0.51	0.28 ± 0.95
<i>Cynoscion</i> spp.	0.04	0.10	0.07 ± 0.42
<i>Larimus fasciatus</i>	0.06	0.32	0.20 ± 0.58
<i>Menticirrhus americanus</i>	-	0.22	0.11 ± 0.50
<i>Micropogonias undulatus</i>	0.25	139.02	71.92 ± 165.22
<i>Sciaenops ocellatus</i>	0.09	7.10	3.71 ± 9.55
Unknown	0.02	2.55	1.33 ± 7.62
Total	0.73	151.83	

Table 7 - Sciaenid species density (fish/100m³) arranged by sampling depth (surface or not surface) resulting in total averaged (mean ± standard deviation). Dash (-) denotes no taxa collected in tow. Data presented is restricted to fall months: September, October, and November.

sciaenid spp.	Net Level Sciaenid Larval Density (fish/100m ³)		
	not surface	surface	Total Averaged (mean ± SD)
<i>Menticirrhus</i> spp.	0.53	0.70	0.61 ± 1.29
<i>Cynoscion arenarius</i>	0.14	0.11	0.12 ± 0.41
<i>Cynoscion nebulosus</i>	0.24	0.04	0.15 ± 0.62
<i>Cynoscion nothus</i>	0.35	0.19	0.28 ± 0.95
<i>Cynoscion</i> spp.	0.10	0.03	0.07 ± 0.42
<i>Larimus fasciatus</i>	0.27	0.09	0.20 ± 0.58
<i>Menticirrhus americanus</i>	0.16	0.05	0.11 ± 0.50
<i>Micropogonias undulatus</i>	104.63	26.30	71.92 ± 165.22
<i>Sciaenops ocellatus</i>	3.75	3.66	3.71 ± 9.55
Unknown	1.77	0.72	1.33 ± 7.62
Total	111.92	31.89	

Table 8 - Sciaenid species density (fish/100m³) arranged by sampling tidal cycle (ingoing or outgoing) resulting in total averaged (mean ± standard deviation). Dash (-) denotes no taxa collected in tow. Data presented is restricted to the fall months: September, October, and November.

sciaenid spp.	Fall Tide Sciaenid Larval Density (fish/100m ³)			Total Averaged (mean ± SD)	
	in	out			
<i>Menticirrhus</i> spp.	0.41	0.98	0.70	±	1.29
<i>Cynoscion arenarius</i>	0.15	0.09	0.12	±	0.41
<i>Cynoscion nebulosus</i>	0.30	-	0.15	±	0.62
<i>Cynoscion nothus</i>	0.48	0.07	0.28	±	0.95
<i>Cynoscion</i> spp.	0.02	0.12	0.07	±	0.42
<i>Larimus fasciatus</i>	0.29	0.09	0.20	±	0.58
<i>Menticirrhus americanus</i>	0.12	0.11	0.11	±	0.50
<i>Micropogonias undulatus</i>	100.47	41.43	71.92	±	165.22
<i>Sciaenops ocellatus</i>	2.00	5.54	3.71	±	9.55
Unknown	0.19	2.55	1.33	±	7.62
Total	104.45	50.98			

3.2.3. Paralichthyid Barcoding Results

Out of 19 individuals barcoded, 12 were correctly identified to species, seen below in Table 9. As only 63% were correctly identified using morphological characteristics further analysis was not completed. Although future barcoding may be completed on all individuals identified as *Paralichthys* in a later analysis.

Table 9- Morphological identification vs. genetic identification of paralichthyids from February sampling.

Vial	Morphological ID	Genetic ID	Identified Correctly
R1	<i>Paralichthys lethostigma</i>	<i>P. lethostigma</i>	Y
R2	<i>Paralichthys lethostigma</i>	<i>P. lethostigma</i>	Y
R3	<i>Paralichthys lethostigma</i>	<i>P. albigutta</i>	N
R4	<i>Paralichthys lethostigma</i>	<i>Citharichthys spilopterus</i>	N
R5	<i>Paralichthys lethostigma</i>	<i>Citharichthys spilopterus</i>	N
R6	<i>Paralichthys lethostigma</i>	<i>P. lethostigma</i>	Y
R7	<i>Paralichthys lethostigma</i>	<i>P. lethostigma</i>	Y
R8	<i>Citharichthys spilopterus</i>	<i>P. lethostigma</i>	Y
R9	<i>Paralichthys lethostigma</i>	<i>P. albigutta</i>	N
R10	<i>Paralichthys lethostigma</i>	<i>P. lethostigma</i>	Y
R11	<i>Paralichthys lethostigma</i>	<i>P. lethostigma</i>	Y
R12	<i>Paralichthys lethostigma</i>	<i>P. lethostigma</i>	Y
R13	<i>Paralichthys lethostigma</i>	<i>P. lethostigma</i>	Y
R14	<i>Paralichthys lethostigma</i>	<i>P. lethostigma</i>	Y
R15	<i>Citharichthys spilopterus</i>	<i>P. lethostigma</i>	N
R16	<i>Citharichthys spilopterus</i>	<i>P. lethostigma</i>	N
R17	<i>Paralichthys lethostigma</i>	<i>P. lethostigma</i>	Y
R18	<i>Paralichthys lethostigma</i>	<i>Citharichthys spilopterus</i>	N
R19	<i>Paralichthys lethostigma</i>	<i>P. lethostigma</i>	Y

3.3. Total Larval Density Community Analysis

The initial model compared total larval density against the four factors (tidal cycle, time of day, depth, and month) and resulted in time of day having the highest f -value (35.2) indicating the largest group separation (Table 10). The model was then split into day only and night only to better understand fine scale patterns within each group. The distribution of the total larval density for each month sampled was significantly larger at night than during the day (Figure 6). The variation between day and night was most apparent in fall months and less apparent in February (Figure 6).

3.3.1. Day Model

The day model resulted in a significant interaction between month and tide thus the day model was split into a one-way model of tide by month, Table 11. Only the months of September ($p < 0.01$) and February ($p < 0.05$) had significant differences between tide (Table 12). In September, ingoing tide had significantly higher densities of larvae than outgoing tide, while in February outgoing tide had significantly higher densities of larvae (Figure 7).

3.3.2. Night Model

The night model resulted in a significant interaction between month and depth stratum, thus the day model was split into a one-way model of depth stratum by month (Table 13). Tide was not included in the night model because of non-significance, which may be due to insufficient sample size. During the months of September, October, and November the non-surface samples had significantly higher densities than the surface samples while in February the surface samples had significantly higher densities (Figure 8). Month and depth stratum had a significant interaction ($p < 0.005$; Table 14; Figure 8).

Table 10 - ANOVA model results for total larval density vs the factors month, time of day, depth of net, and tidal cycle. Showing degrees of freedom (df), *f*-value, and *p*-values.

Full Model Total Larval Density			
	df	<i>f</i> -value	<i>p</i> -value
(Intercept)	1	15.100	< 0.001
Month	3	4.693	0.004
Time_Day	1	35.215	< 0.001
Depth_Stratum	1	14.109	< 0.001
Tide	1	12.000	< 0.001
Month:Time_Day	3	9.248	< 0.001
Month:Depth_Stratum	3	9.809	< 0.001
Month:Tide	3	9.141	< 0.001
Time_Day:Depth_Stratum	1	8.859	0.004
Time_Day:Tide	1	1.044	0.309
Depth_Stratum:Tide	1	0.049	0.826

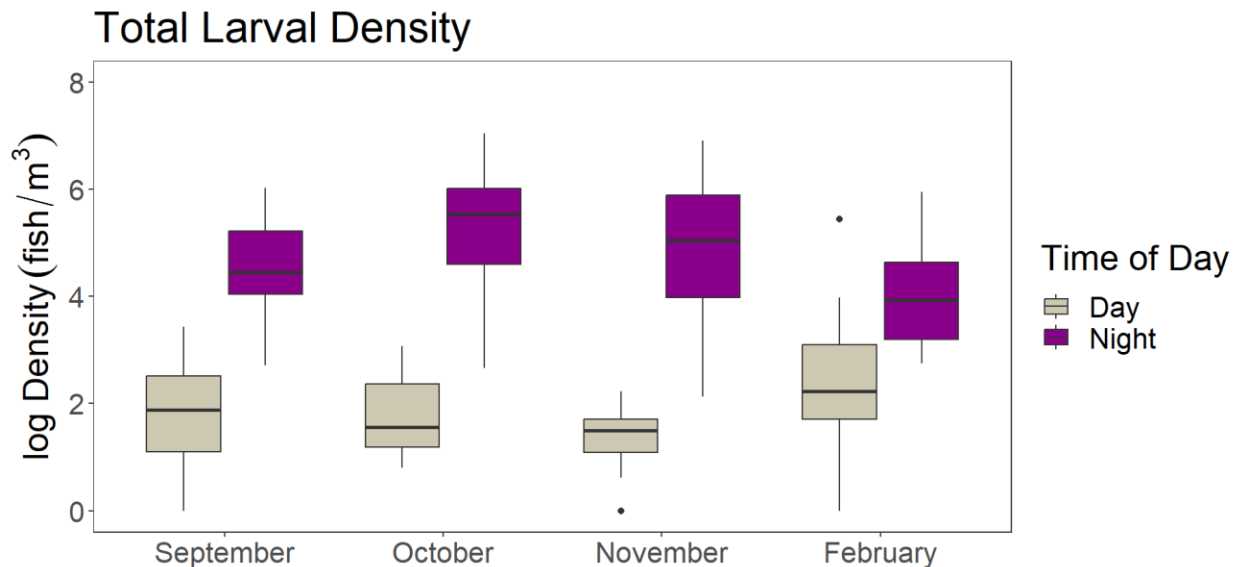


Figure 6 - Median total ichthyoplankton densities (fish/ 100m³) captured during the day (grey) and night (purple) for September, October, November, and February. Ichthyoplankton densities were log transformed. The lower and upper boxes correspond to the first and third quartiles, while the whiskers extend to no larger than 1.5 times the interquartile range (IQR). The black points indicate values that fell out of the IQR (outliers).

Table 11 - ANOVA model results for total larval density collected during the day vs the factors month, depth of net, and tidal cycle. Showing degrees of freedom (df), *f*-value, and *p*-values.

Day Model: Total Larval Density			
	DF	<i>f</i> -value	<i>p</i> -value
(Intercept)	1	260.207	< 0.001
Month	3	4.901	0.005
Depth Stratum	1	0.066	0.798
Tide	1	0.053	0.820
Month:Depth Stratum	3	2.591	0.064
Month:Tide	3	7.604	< 0.001
Depth Stratum:Tide	1	0.584	0.449

Table 12 - ANOVA model results for total larval density collected during the day grouped by month vs the factors of tidal cycle. Showing degrees of freedom (DF), *f*-value, and *p*-values.

Tide-Month Model: Total Larval Density			
	DF	<i>f</i> -value	<i>p</i> -value
September			
(Intercept)	1	72.807	< 0.001
Tide	1	15.160	0.002
October			
(Intercept)	1	77.863	< 0.001
Tide	1	0.078	0.784
November			
(Intercept)	1	75.630	< 0.001
Tide	1	1.941	0.189
February			
(Intercept)	1	61.853	< 0.001
Tide	1	5.157	0.038

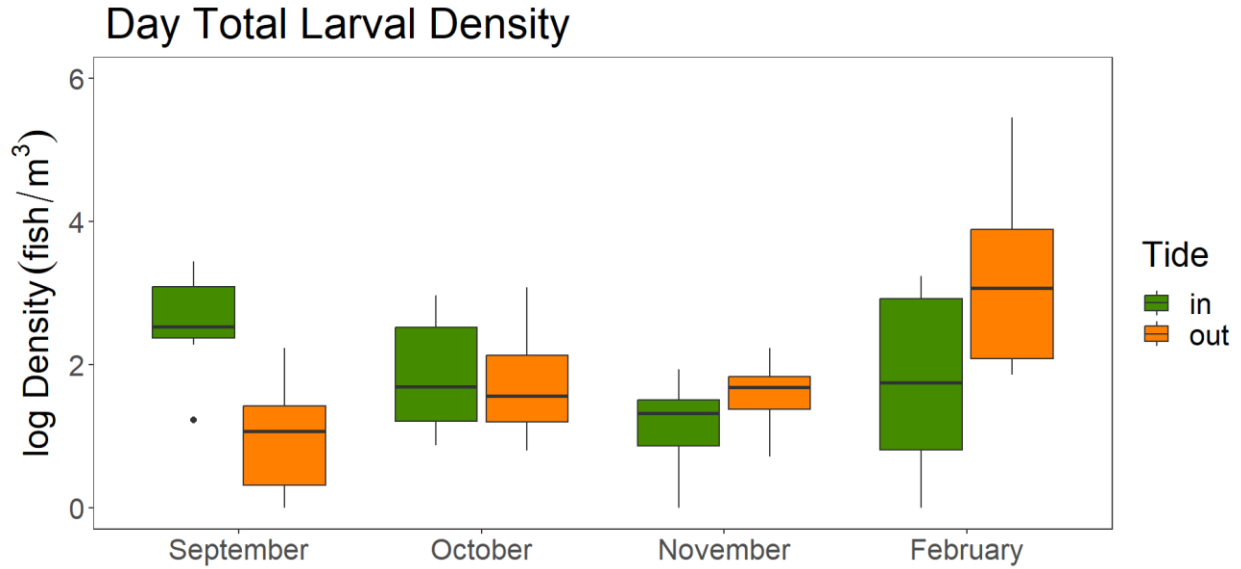


Figure 7 - Median total ichthyoplankton densities (fish/ 100m³) captured during ingoing tide (green) and outgoing tide (orange) for samples collected during the day. Ichthyoplankton densities were log transformed. The lower and upper boxes correspond to the first and third quartiles, while the whiskers extend to no larger than 1.5 times the interquartile range (IQR). The black points indicated values that fell out of the IQR (outliers).

Table 13 - ANOVA model results for total larval density collected during the night vs the factors month, depth of net, and tidal cycle. Showing degrees of freedom (DF), f-value, and p-values.

Night Model: Total Larval Density			
	DF	<i>f</i> -value	<i>p</i> -value
(Intercept)	1	1383.904	< 0.001
Month	3	4.213	0.009
Depth Stratum	1	12.665	< 0.001
Month:Depth Stratum	3	12.218	< 0.001

Table 14 - ANOVA model results for total larval density collected during the night grouped by month vs the factors of net depth. Showing degrees of freedom (DF), *f*-value, and *p*-values.

Month vs Depth Model: Total larval Density			
	DF	<i>f</i> -value	<i>p</i> -value
September			
(Intercept)	1	171.841	< 0.001
Depth Stratum	1	4.320	0.092
October			
(Intercept)	1	97.738	< 0.001
Depth Stratum	1	1.802	0.187
November			
(Intercept)	1	126.256	< 0.001
Depth Stratum	1	0.747	0.393
February			
(Intercept)	1	132.285	< 0.001
Depth Stratum	1	1.571	0.219

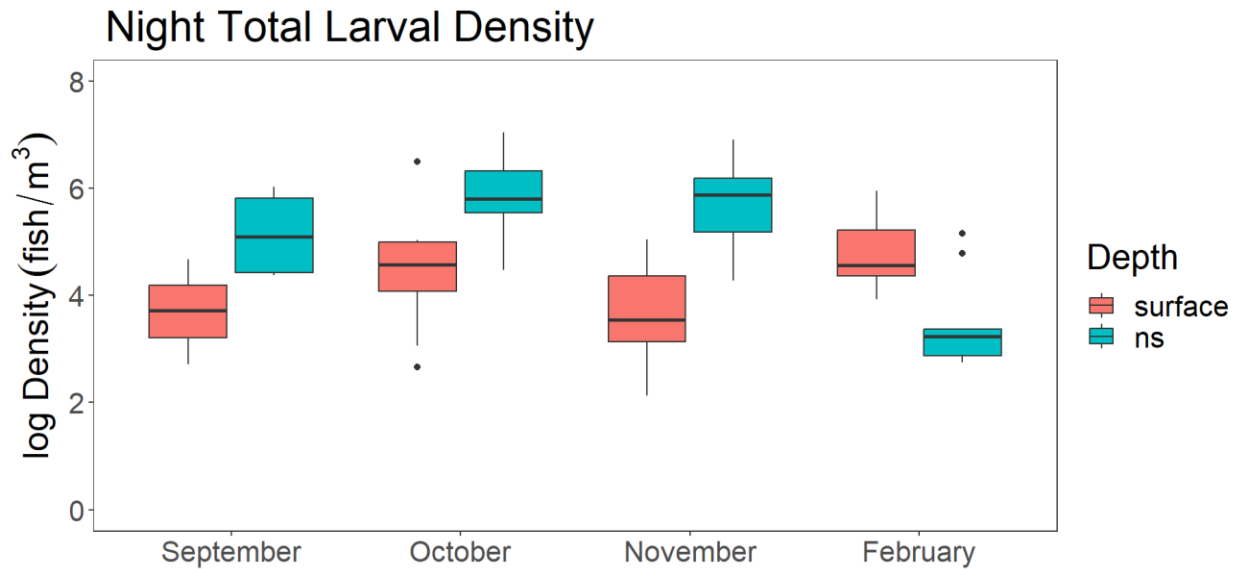


Figure 8 - Median total ichthyoplankton densities (fish/ 100m³) captured at surface depths (red) and non-surface depths (blue; ns) for samples collected during the night. Ichthyoplankton densities were log transformed. The lower and upper boxes correspond to the first and third quartiles, while the whiskers extend to no larger than 1.5 times the interquartile range (IQR). The black points indicated values that fell out of the IQR (outliers).

3.4. Family Density Analysis

3.4.1. Sciaenidae

The sciaenid model showed a significant relationship between larval density and time of day as well as the interaction between time of day and depth (Table 15). The Sciaenidae model was then broken down into a day-time model and night-time model because that factor had the largest f -value (75.77) and thus indicating the most group separation. There was a significant difference ($p < 0.05$) in larval density due to the interaction between time of day and depth. As seen in Tables 5 – 8, the majority of identified sciaenids were *M. undulatus* (Atlantic croaker) indicating that the results of the sciaenid analysis are driven by *M. undulatus*, with higher larval densities occurring at night and non-surface depths (Figure 9).

The day model showed a significant difference in larval density based on depth, with higher larval densities occurring at mid and bottom tows (Table 16). This difference was consistent across both ingoing and outgoing tides but more apparent during the outgoing tide (Figure 10). There was no significant interaction between tide and depth.

The night sciaenid model shows a significant difference ($\alpha < 0.05$) in larval density based on the interaction between tide and depth (Table 17), with higher densities occurring at non-surface depths for both tidal cycles but only significantly higher densities occurring during outgoing tide for non-surface depths (Figure 11).

Table 15 - ANOVA model results for Sciaenid larval density vs the factors month, time of day, depth of net, and tidal cycle. Showing degrees of freedom (DF), f-value, and p-values.

Full Model: Sciaenidae Larval Density			
	DF	f-value	p-value
(Intercept)	1	3.056	0.084
Time of Day	1	75.772	< 0.001
Depth	1	1.132	0.291
Tide	1	0.012	0.915
Time of Day:Depth	1	4.862	0.030
Time of Day:Tide	1	0.596	0.442
Depth:Tide	1	0.022	0.884

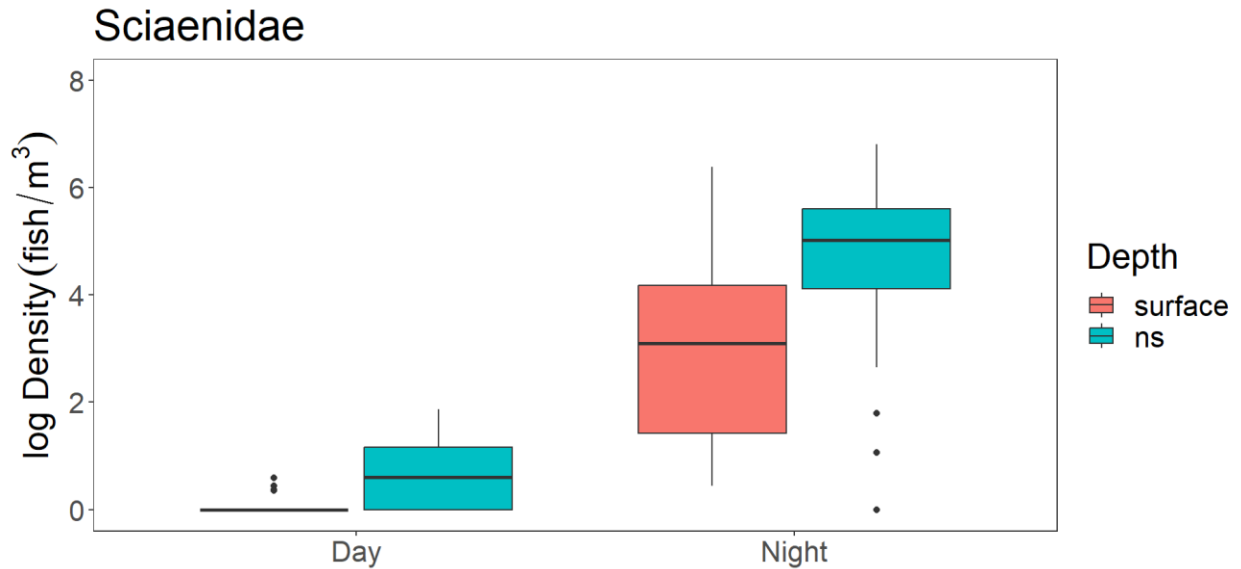


Figure 9 - Median total sciaenid densities (fish/ 100m³) captured at surface depths (red) and non-surface (ns) depths (blue). Sciaenid densities were log transformed with data restricted to fall months (September, October, and November). The lower and upper boxes correspond to the first and third quartiles, while the whiskers extend to no larger than 1.5 times the interquartile range (IQR). The black points indicated values that fell out of the IQR (outliers).

Table 16 - ANOVA model results for sciaenid larval density collected during the day vs the factors depth of net and tidal cycle. Showing degrees of freedom (DF), *f*-value, and *p*-values.

Day Model: Sciaenidae Larval Density			
	DF	<i>f</i> -value	<i>p</i> -value
(Intercept)	1	16.415	< 0.001
Depth	1	4.910	0.032
Tide	1	0.078	0.781
Depth:Tide	1	0.103	0.749

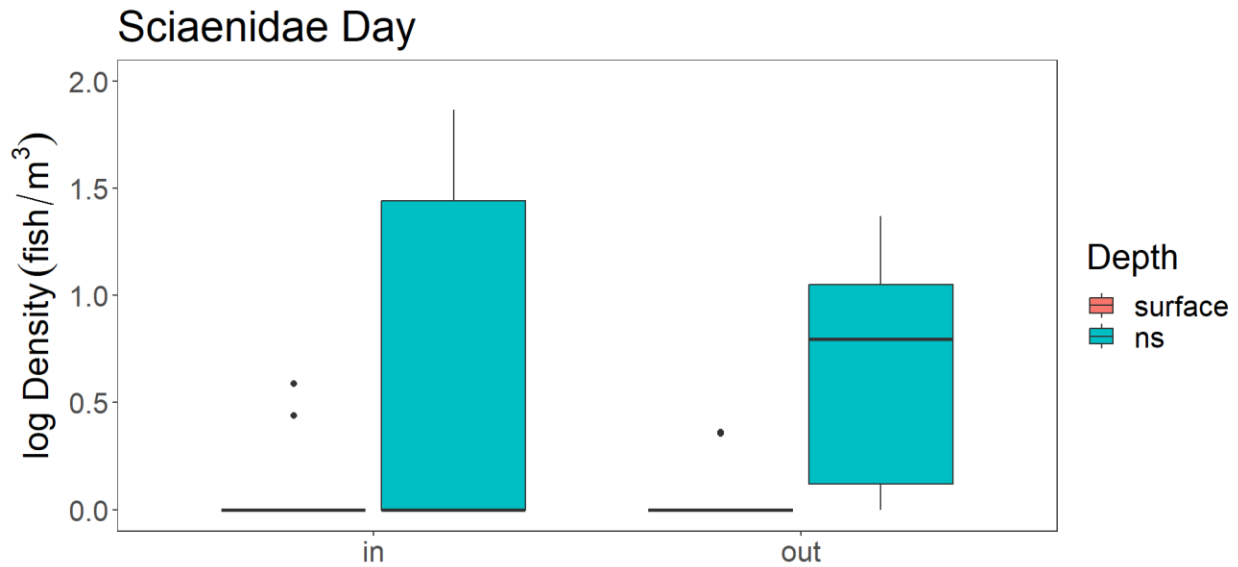


Figure 10 - Median sciaenid densities (fish/ 100m³) captured at surface depths (red) and non-surface depths (blue) for samples collected during the Day with data restricted to fall months (September, October, and November). Sciaenid densities were log transformed. The lower and upper boxes correspond to the first and third quartiles, while the whiskers extend to no larger than 1.5 times the interquartile range (IQR). The black points indicated values that fell out of the IQR (outliers).

Table 17 - ANOVA model results for sciaenid larval density collected during the night vs the factors depth of net and tidal cycle. Showing degrees of freedom (DF), *f*-value, and *p*-values.

Night Model: Sciaenidae Larval Density			
	DF	<i>f</i> -value	<i>p</i> -value
(Intercept)	1	28.409	< 0.001
Depth	1	6.649	0.014
Tide	1	0.249	0.620
Depth:Tide	1	0.003	0.954

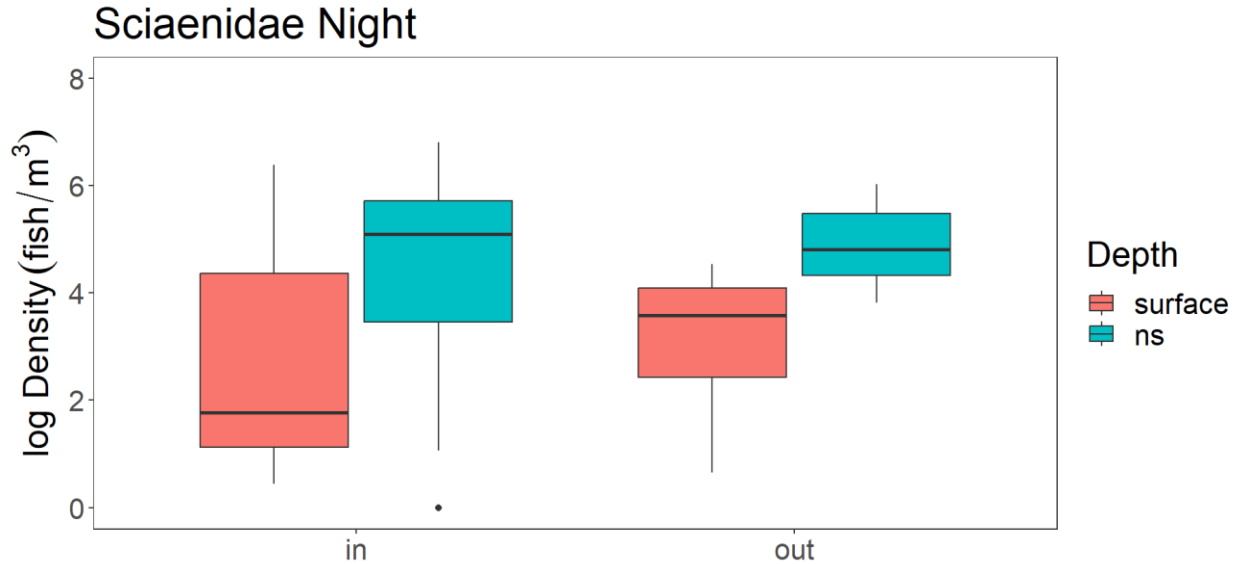


Figure 11- Median total sciaenid densities (fish/ 100m³) captured at surface depths (red) and non-surface depths (blue) for samples collected during the night with data restricted to fall months (September, October, and November). Sciaenid densities were log transformed. The lower and upper boxes correspond to the first and third quartiles, while the whiskers extend to no larger than 1.5 times the interquartile range (IQR). The black points indicated values that fell out of the IQR (outliers).

3.5. Family PCA

Increased densities of sciaenids were observed in the months October and November, while an increase in clupeid density was positively correlated with the month October, and an increase in sparid density with February (Figure 17, Figure 18). Gobiid density had a possible positive correlation with September, but the correlation is not as apparent as with the other families (Figure 17, Figure 18). There was little correlation between tidal cycle and family densities, although there was an increase in sparid density associated with outgoing tide (Figure 19, Figure 20). A positive correlation between density and night (Figure 21, Figure 22) was found for all four families (Sciaenidae, Clupeidae, Gobiidae, and Sparidae). Sciaenid, clupeid, and gobiid densities were positively correlated with non-surface depths, while sparid density was positively correlated with surface depths (Figure 23, Figure 24).

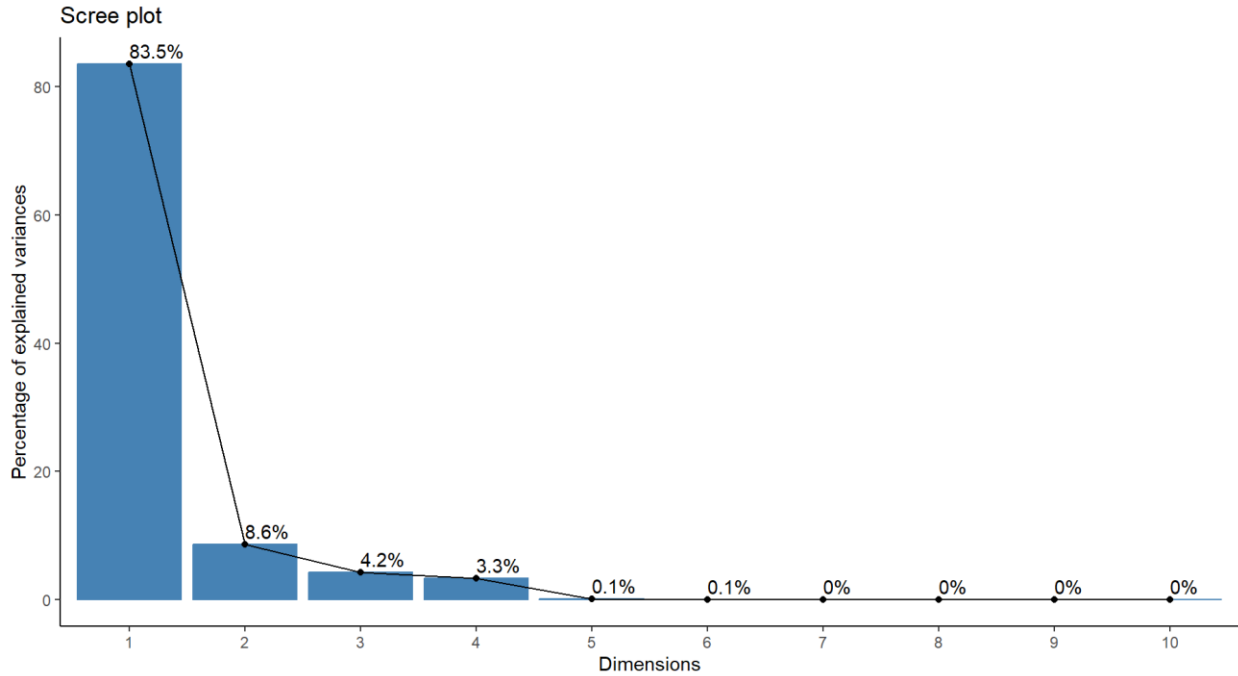


Figure 12 - Scree plot of PCA of family densities. 83.5% of the variance in the data is explained by the first dimension. A total of 99.6% of the variance in the data is explained by the first four dimensions.

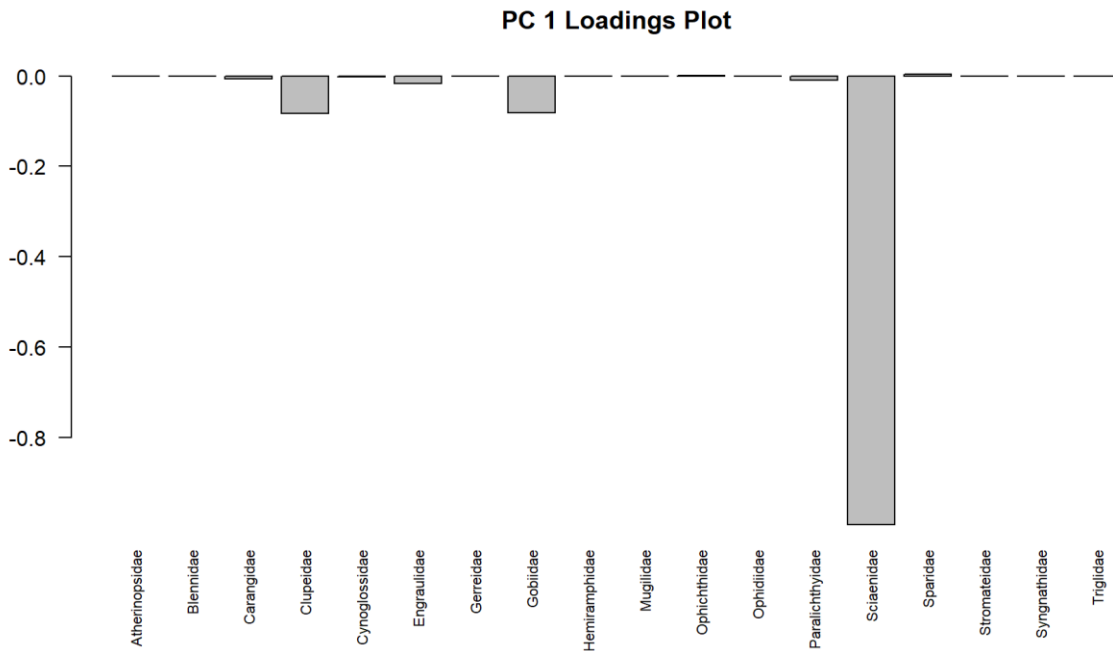


Figure 13 - Loadings plot for principal component 1. Sciaenids, gobiids, and clupeids had the largest influence of PC1.

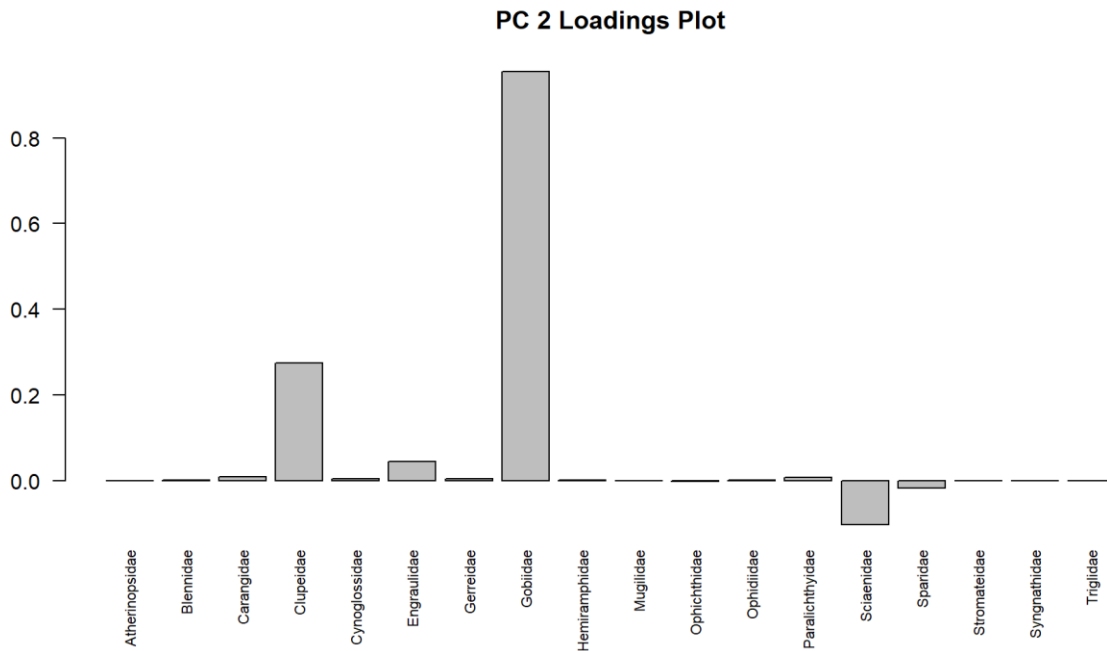


Figure 14 - Loadings plot for principal component 2. Gobiids, clupeids, and sciaenids had the largest influence of PC2.

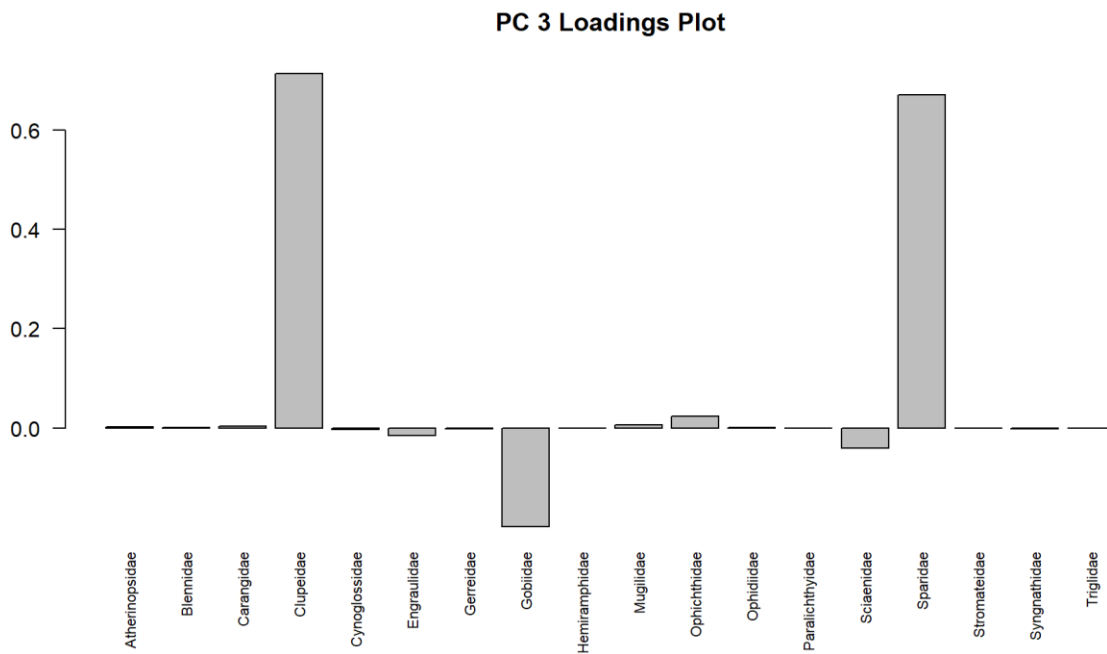


Figure 15 - Loadings plot for principal component 3. Clupeids, sparids, and gobiids had the largest influence of PC3.

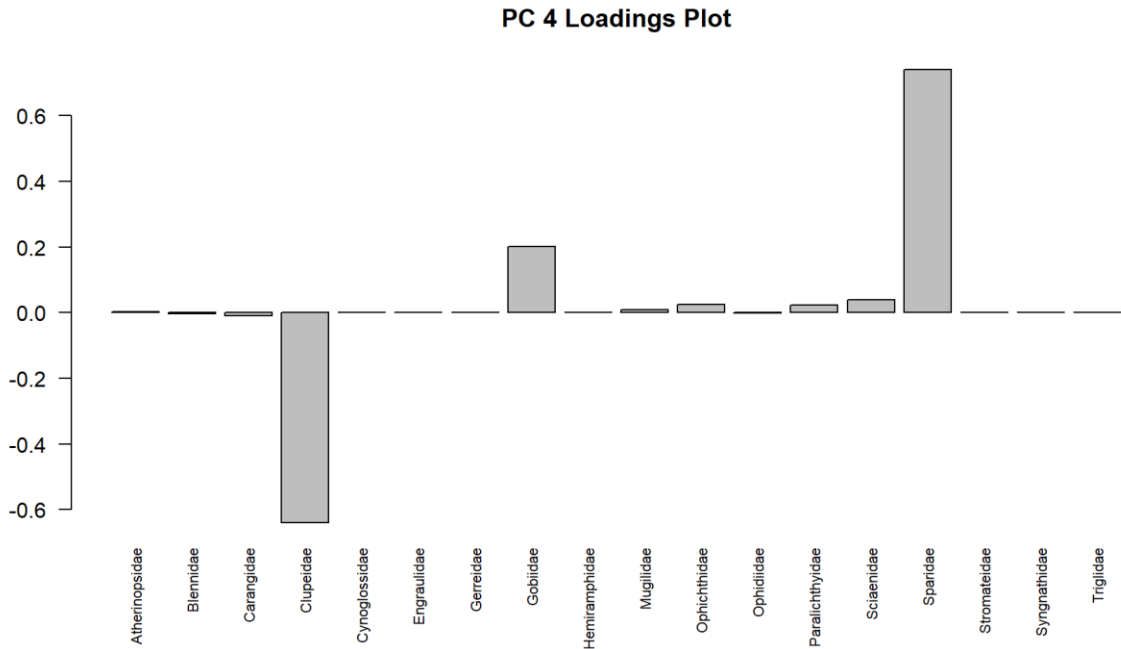


Figure 16 - Loadings plot for principal component 4. Sparids, clupeids, and gobiids had the largest influence of PC4.

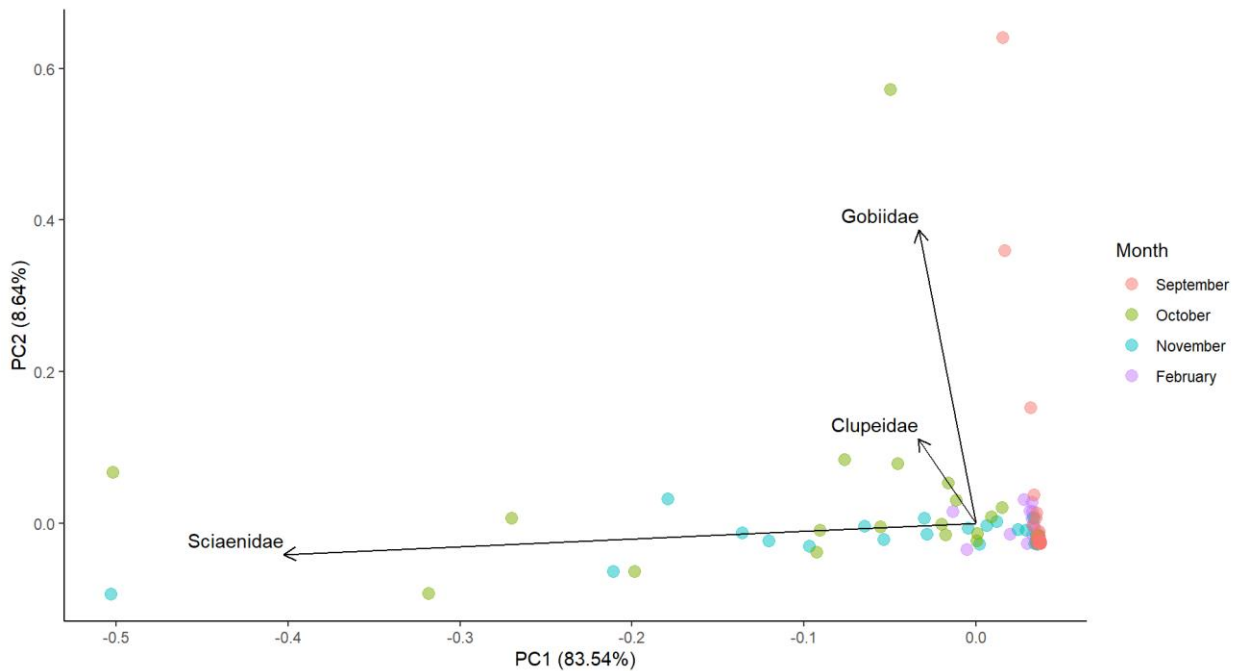


Figure 17 - PCA biplot for PC1 and PC2. Points are colored by month (September, October, November, and February) and loading vectors indicate an increase in family density. Families displayed correspond to the families that contributed the most to PC1 and PC2.

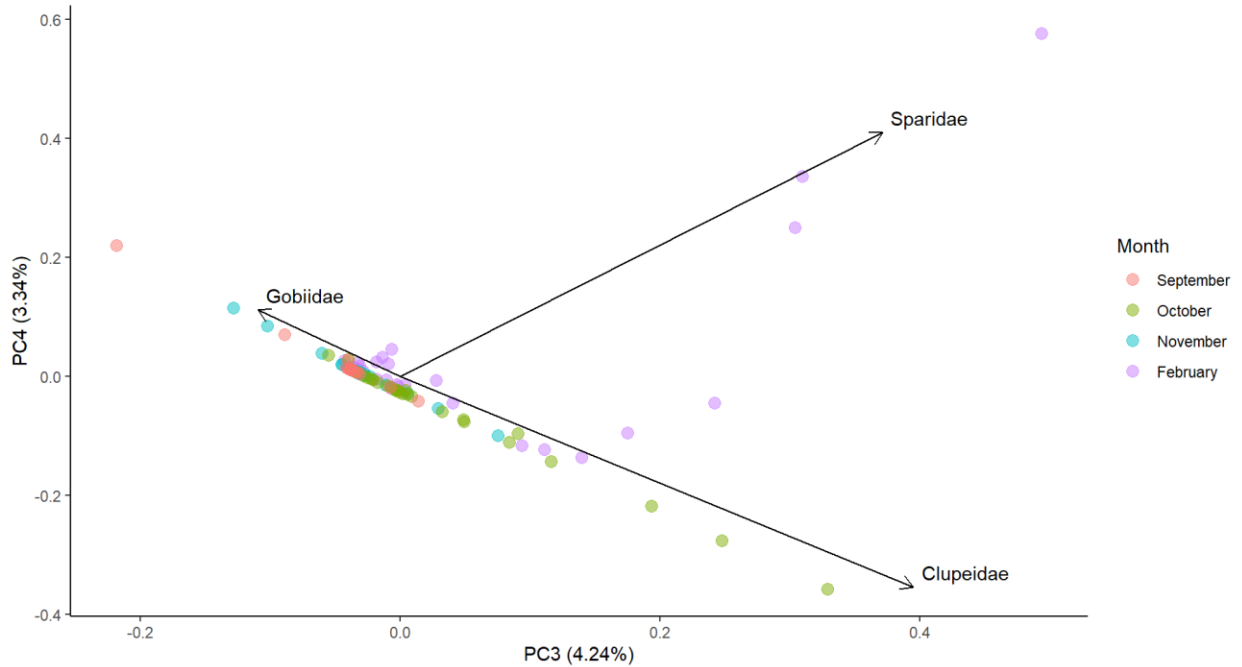


Figure 18 - PCA biplot for PC3 and PC4. Points are colored by month (September, October, November, and February) and loading vectors indicate an increase in family density. Families displayed correspond to the families that contributed the most to PC3 and PC4.

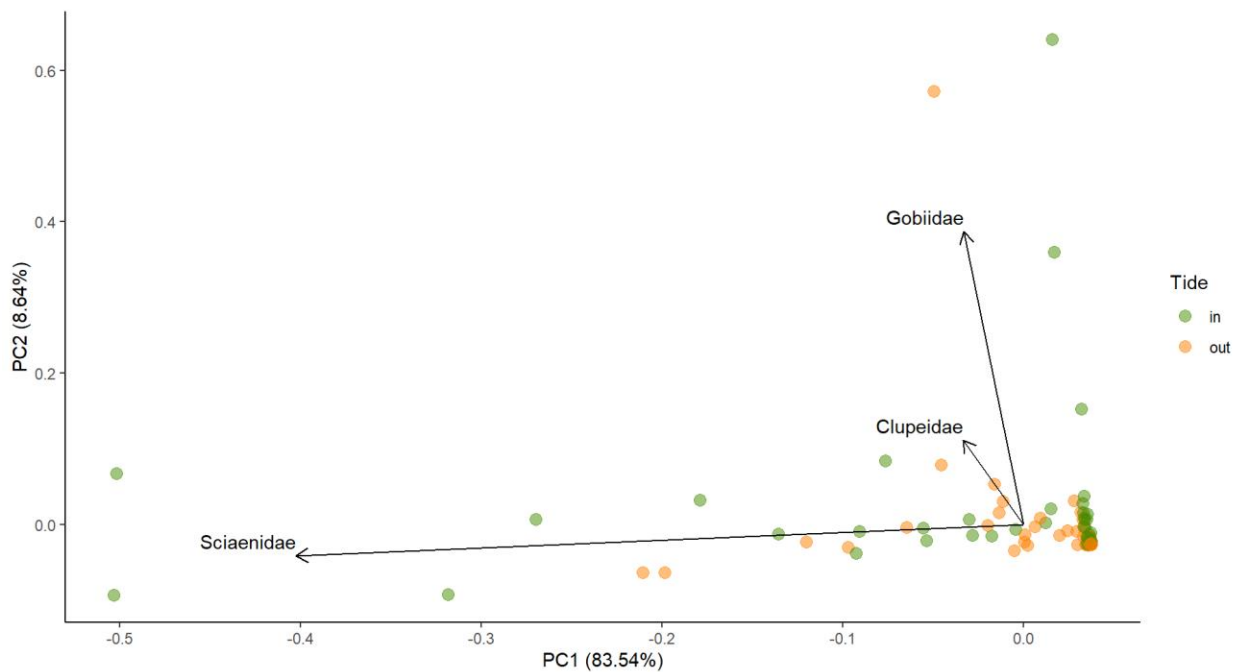


Figure 19 - PCA biplot for PC1 and PC2. Points are colored by tidal cycle (ingoing and outgoing) and loading vectors indicate an increase in family density. Families displayed correspond to the families that contributed the most to PC1 and PC2.

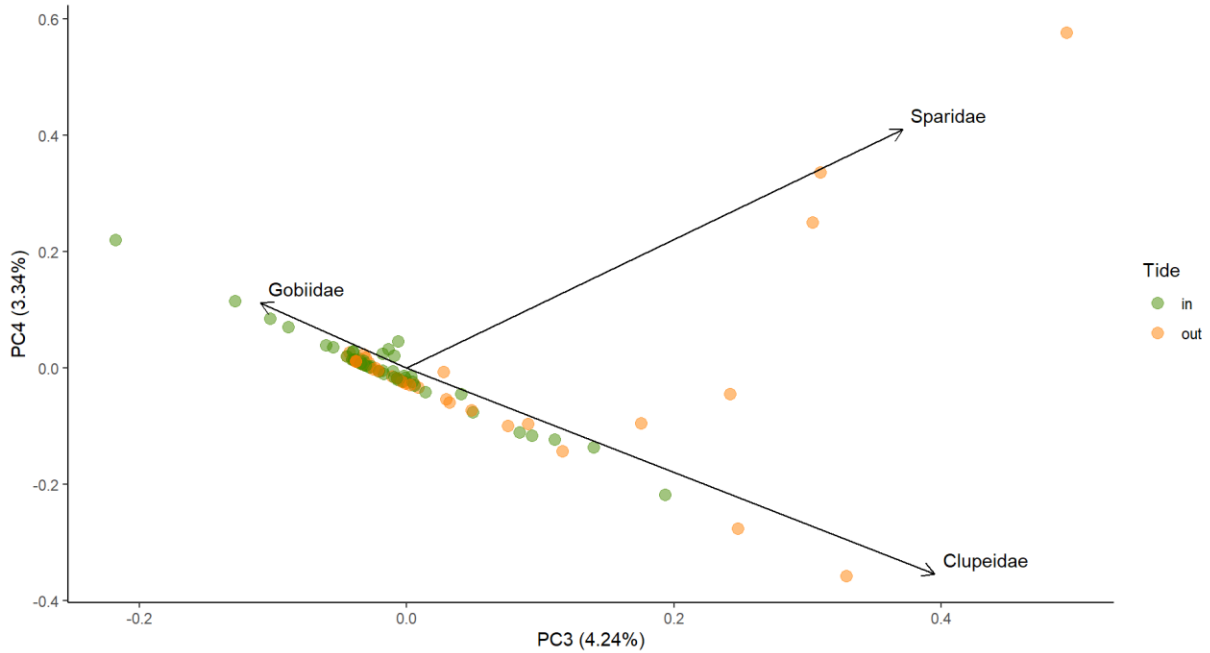


Figure 20 - PCA biplot for PC3 and PC4. Points are colored by tidal cycle (ingoing and outgoing) and loading vectors indicate an increase in family density. Families displayed correspond to the families that contributed the most to PC3 and PC4.

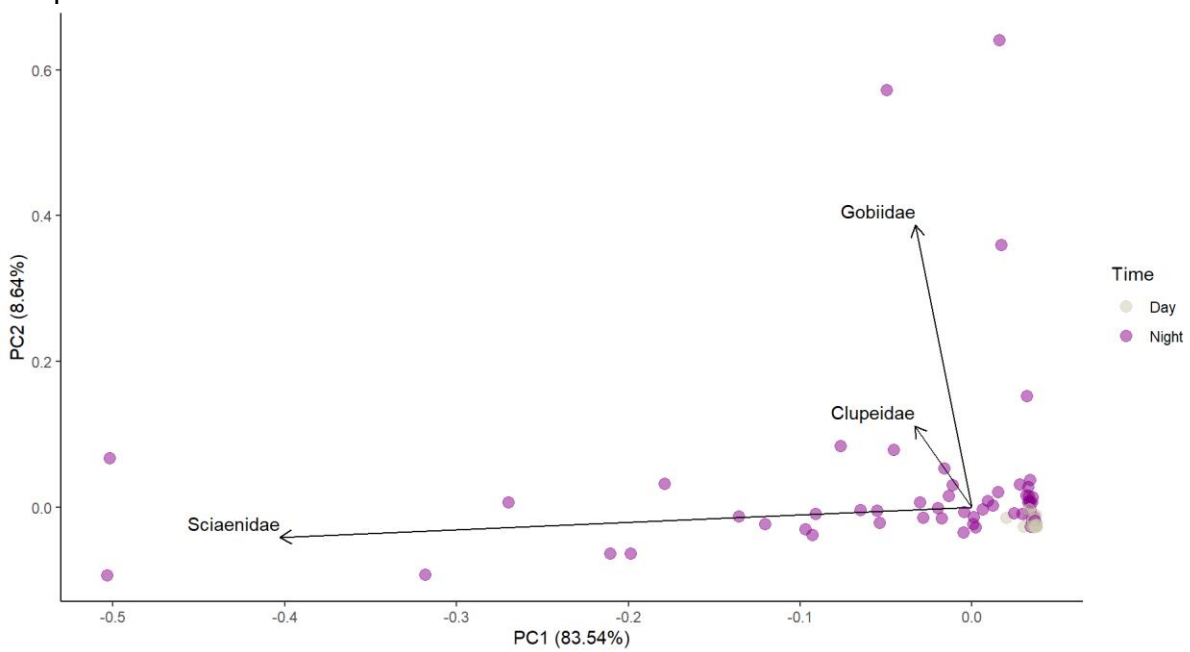


Figure 21 - PCA biplot for PC1 and PC2. Points are colored by photoperiod (day and night) and loading vectors indicate an increase in family density. Families displayed correspond to the families that contributed the most to PC1 and PC2.

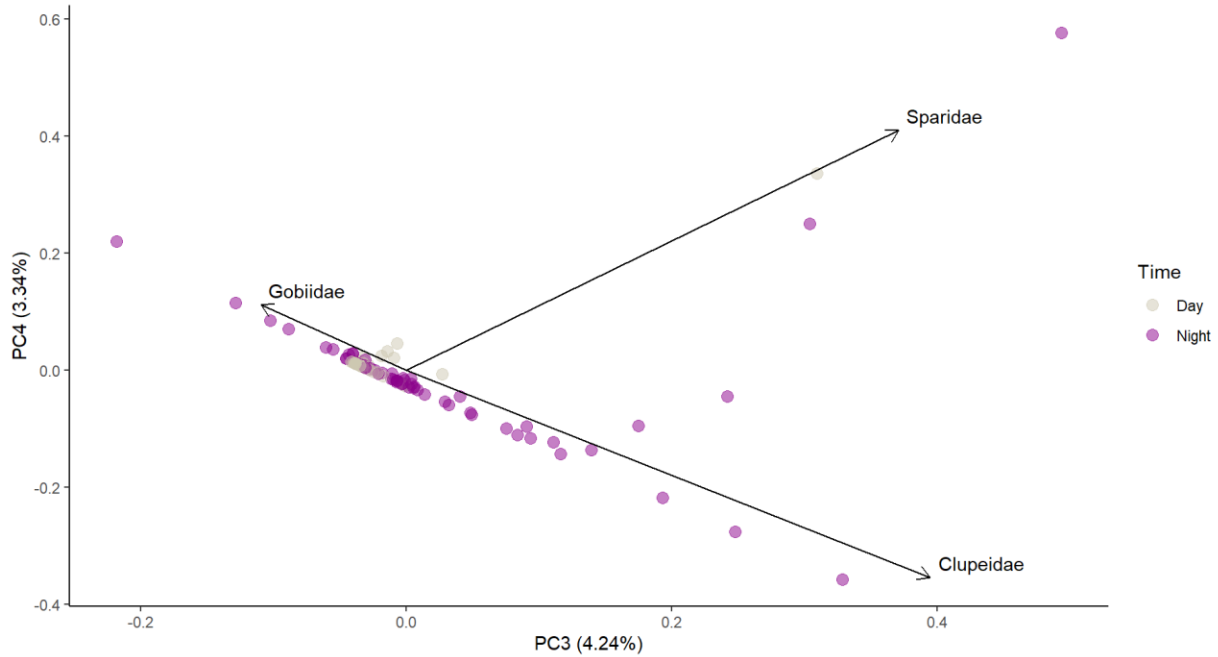


Figure 22 - PCA biplot for PC3 and PC4. Points are colored by photoperiod (day and night) and loading vectors indicate an increase in family density. Families displayed correspond to the families that contributed the most to PC3 and PC4.

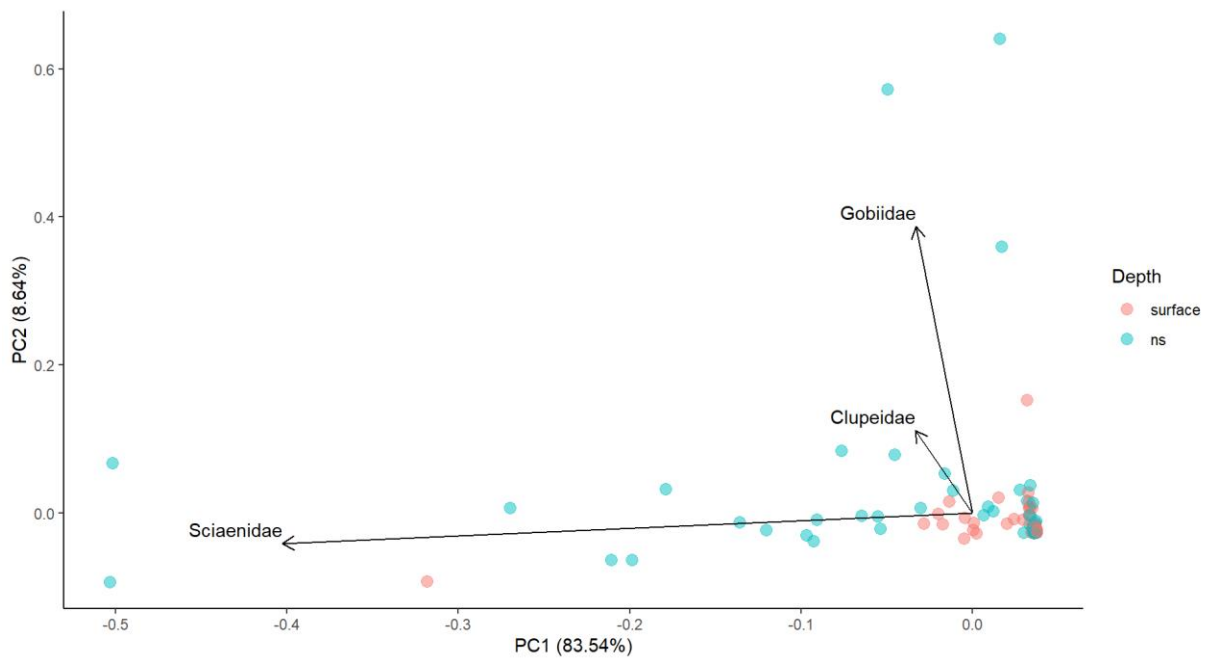


Figure 23 - PCA biplot for PC1 and PC2. Points are colored by depth stratum (surface and non-surface) and loading vectors indicate an increase in family density. Families displayed correspond to the families that contributed the most to PC1 and PC2.

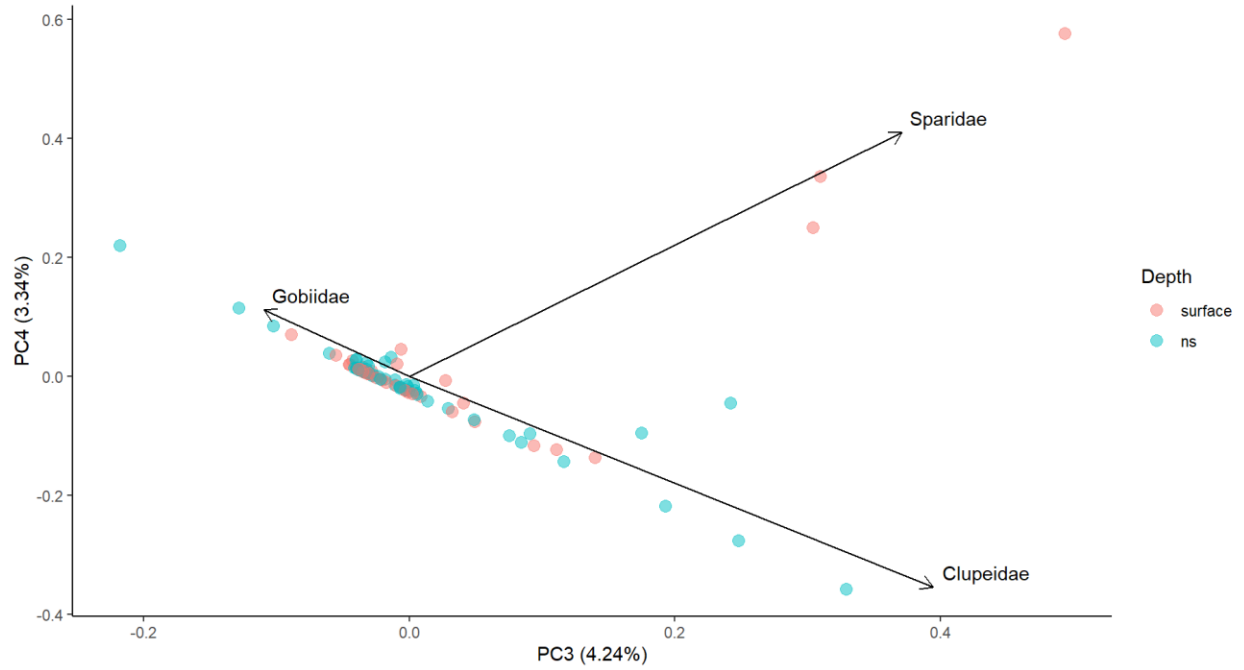


Figure 24 - PCA biplot for PC3 and PC4. Points are colored by depth stratum (surface and non-surface) and loading vectors indicate an increase in family density. Families displayed correspond to the families that contributed the most to PC3 and PC4.

4. DISCUSSION

4.1. Ichthyoplankton Community

The result of family and sciaenid species composition analyses were consistent with previous research in coastal bays and estuaries of southern Texas (Tolan et al., 1997; Tolan, 2008). The highest density of ichthyoplankton occurred in the fall with most individuals being from the family Sciaenidae, which is supported by previous research in the region (Hall et al., 2019). The majority of individuals collected in the months of October and November were *M. undulatus* (Atlantic croaker). The timeframe in which *M. undulatus* spawns vary with latitude, with summer/fall spawning occurring in more northern latitudes and fall/winter spawning occurring in more southern latitudes (White & Chittenden, 1977; Ross, 1988), a phenomenon linked to photoperiod-temperature regime shifts (Khan & Thomas, 1996). Although the timeframe of *M. undulatus* spawning varies, the results seen in this paper correspond to their recorded spawning peak in fall/winter in the GOM (Anderson et al., 2018; Richards, 2005; Holt et al., 1985). *S. ocellatus*, another member of the sciaenid family, was also abundant in October and November, again consistent with known spawning times in the GOM (Peters & McMichael, 1987). In September, the most abundant family was Gobiidae, aligning with spawning times of gobies, primarily *Gobisoma bosc* (Dahlberg & Conyers, 1973). Finally, during February, clupeids and sparids were the most abundant, likely corresponding to the spawning times of *Brevoortia patronus* (Gulf menhaden) and *Lagodon rhomboides* (pinfish) respectively (Lassuy, 1983; Richards, 2005). Spawning times of fishes are known to correlate with shifts in environmental parameters including temperature, diel cycle duration, salinity, and current direction and speed (Lowerre-Barbieri et al., 2011) related to the change in seasons, summer to fall or fall to winter for example (Lowerre-Barbieri et al., 2011). In the study area, the environmental parameters shift from

warm, salty waters in the summer to cooler, fresher waters in the winter (Figure 3). Furthermore, spawning time of a species in the same geographical area can vary on a yearly basis. Cooler temperatures in November and December have been linked to earlier migration of multiple species of adults of spring spawning species in the North Sea to offshore waters while summer spawners showed earlier migration with warmer temperatures in March (Genner et al., 2010). This temperature related early migration to offshore spawning locations could be a possible trigger for earlier spawning times (Sims et al., 2004; Genner et al., 2010). It is possible that a similar temperature driven migration occurs in the coastal waters of Texas as well.

4.2. Ichthyoplankton Transportation

This study focused on transportation of the larval stage of particular species, which spawn offshore and use inshore for nursery habitat, primarily sciaenids and paralichthyids (specifically southern flounder, *P. lethostigma*). While several individuals were identified as *P. lethostigma*, the number was not large enough to do a robust ANOVA as was the case with the sciaenids. Targeting the spawning timeframe of *P. lethostigma* would make a more ideal data set for analysis. With these factors in mind, the interpretation of the results will focus primarily on the months (October and November) and during night hours, in which sciaenids were found to be the most abundant family.

Analysis of total larval density indicated higher densities at night and during the months of October and November. During the day, density varied based on the interaction of month and tide, whereas the night density varied based on the interaction between month and depth. The density data analysis of sciaenids paralleled that of the total larval density during the months of October and November. With significantly higher densities of sciaenids occurring at night and non-surface depths.

Lower densities during daylight hours may indicate a predator avoidance strategy and/or avoidance of damaging UV rays. Both theories are commonly referred to when discussing diel vertical migration (DVM) of larval fishes (Lampert, 1989; Hays, 2003). Although, this study recorded higher total larval densities at night occurred in non-surface waters (September, October, and November) and there was no significant difference in total larval density through depth during the day, which does not align with DVM. It is possible that there is some correlation between environmental factors and density which we were unable to identify due to the low densities of ichthyoplankton collected during the day. In another study, Hernandez et al. (2009) found that high turbulence in surface waters, caused by wind forcing, corresponded to ichthyoplankton's vertical movement to deeper waters. Substantial ship traffic is also responsible for increased turbidity, creating an artificial upwelling effect which resuspends sediment in the surrounding waters (Irvine et al., 1997; Lindholm et al., 2001). Finally dredging is another practice which increases the turbidity in the aquatic environment, as substrate is removed to increase depth for ship movement (Erfteimeijer & Lewis, 2006). As wind and ship traffic play an important role in coastal waters of Texas, the avoidance of turbulent surface waters may also explain ichthyoplankton vertical distributions. Turbulent waters are known to correspond to lower densities of larval fish, primarily because of reduced feeding success, specifically in the coastal waters of Texas (Lunt & Smee, 2014). This may in part explain why fewer fish were collected during daytime, when there is heavy ship traffic, as compared to the night when more fish were observed and ship traffic was greatly reduced. Future research should be conducted to investigate the effect of turbulent surface waters on ichthyoplankton movement, especially in the coastal waters of Texas.

Net avoidance and gear restrictions may further account for the low number of individuals collected during the day. In a study conducted by Thayer et al. (1983), higher densities of

ichthyoplankton were collected during the day, were obtained using a high-speed sampling technique rather than using a standard bongo net. During daylight hours larvae may easily be able to visually perceive the net and actively avoid the net due to slow standard sampling speeds. However, this theory assumes that (1) the larval fish are adequately developed to be able to swim faster than the sampling gear (2) the sampled waters have low turbidity thus improving visual acuity.

Water quality data (salinity, temperature, oxygen, and pH) indicated a mixed water column, for most sampling rounds, making it hard to draw conclusions to support or refute the Sense Acuity and Behavior (SAAB) and the Selective Tidal Stream Transport (STST) theories. SAAB hypothesizes that ichthyoplankton use vertical salinity discrepancies to cue transportation and vertical movement. Even though little of our data was found to directly support SAAB there are still possibilities that allow for SAAB to occur in the studied area, one being that the salt wedge occurred mostly outside of the sampling. Evidence of a salt wedge is seen in some of the deeper stations, PA1 & CC1, (Figure B, D, F, & H) and sciaenids did show a significant change in density with the interaction between tide and depth, indicating this family could be associated with saltier bottom waters. Although there is the possibility that SAAB occurred and was undetected in total larval analysis by this research, other studies have also found a lack of evidence for SAAB. Similar to our results, Baptista et al. (2019) explored *Diplodus sargus* (white seabream) larvae's response to environmental cues, found that the larvae did not show a preference for decreased salinity or increased water temperature, cues which are associated with coastal areas. Instead, exploratory behavior increased with ontogeny (Baptista et al., 2019), likely corresponding to the development of sensory organs. This increase in exploratory behavior could indicate that the larvae were searching for other environmental cues not identified by Baptista et al. (2019), such as the

previously described visual cues or oceanic currents. Similar to SAAB, STST is another theory attributed to the active transportation of ichthyoplankton (Gibson & Atkinson, 2001). Generally, flood tide transportation has been exhibited in ichthyoplankton such as *Brevoortia tyrannus* (Atlantic menhaden) and *P. lethostigma* (Gibson & Atkinson, 2001). Our results found some evidence in support of STST, associating tidal cycle with changes in larval density. An increase in total larval density during the day in the month of September was associated with ingoing tide. Looking further into the results, the PCA reveal an increase in sciaenid density with ingoing tide and an increase in clupeid and sparid density with outgoing tide.

4.3. Implications for Management: Possible Environmental Effects

Desalination plants require water intake systems which result in harmful effects to smaller organisms, such as ichthyoplankton, which are susceptible to impingement. In 2004, legislation was passed updating the requirements for existing facilities, which intake cooling waters, to reduce the mortality of impinged organisms of all life stages (USEPA, 2004). Previously the industry standard was an intake mesh size of 9.5 mm which was solely aimed at reducing the impingement of adults and juvenile organisms and resulted in 80% or larger mortality rate of impinged ichthyoplankton (USA EPA, 2004). These regulations are specified for cooling water intake systems which do not include desalination plants. Because desalination is considered a newer methodology in the United States, many regulations are not yet promulgated to address the unique issues presented by desalination technology and regulations specified for desalination plants are likely to be based upon the regulations for cooling water systems.

Desalination plants further require the placement of wastewater discharge systems and the wastewater produced is a brine often released at high velocities in attempts to acclimatize the wastewater with the environmental conditions. Ichthyoplankton are sensitive to changes in the

environment including salinity, temperature, and current velocity as they are not yet fully developed and are experiencing a period of high growth rate (Faria et al., 2006; Zhang et al., 2022). These rapid changes in the environment can lead to a multitude of complex physiological changes that can vary across species and geographical region (Pankhurst & Munday, 2011). Increased temperature can cause an increase in metabolic rate leading to a higher demand for food resources and thus a higher chance of starvation (Pankhurst & Munday, 2011; Shelley & Johnson, 2022). Changes in salinity also increase metabolic demand in larval fish, even in euryhaline species that are considered tolerant of increased salinities as juveniles and adults (Boeuf & Payen, 2001; Martin & Esbaugh, 2021). In *S. ocellatus*, Ackerly et al. (2023) found that persistent increases in salinity can cause increased mortality, reduced body size and reduced visual acuity. Some of these negative effects on larval *S. ocellatus* were seen at salinities as low as 37.7, as compared to salinities of desalination plant discharges that reach up to 70-80 (Dupavillon & Gillanders, 2009). In our study, significantly larger densities of ichthyoplankton were found at non-surface depths, meaning that a discharge pipe located along the seafloor has the capacity to affect the majority of ichthyoplankton, particularly sciaenids. Locating the discharge further offshore would reduce the possibility of negatively affecting the high concentration of ichthyoplankton traveling through inlets. If the discharge pipe is placed within an inlet, the restriction of discharge timing, depth and volume could limit the negative effects to the ichthyoplankton, because timing, on both daily and yearly scales, as well as water column depth had significant correlations with ichthyoplankton densities.

4.4. Summary & Conclusions

In coastal communities' revenues from fishing activities are vital to the economy. In coastal Texas species of particular economic importance belong to the family Sciaenidae (drums) with over 50% of the Texas recreational fishing industry profit resulting from two sciaenid species, *S.*

occelatus and *C. nebulosus* (Vega et al., 2011; Ackerly et al., 2023). Several sciaenid species such as *M. undulatus* and *S. ocellatus*, in the coastal Texas area migrate offshore to spawn. Once spawning is complete, larvae are transported through coastal inlets into estuaries that act as critical nursery habitat, supporting the growth and development of fishes during their early life stages. The precise mechanism for larval transportation into estuaries remains unclear but from ichthyoplankton studies, including this one, we can gain a better understanding of the relationship between larval density and environmental factors. Not only has this study documented the high biodiversity in the Coastal Texas area by identifying species belonging to 21 families but has also identified predictable patterns of high ichthyoplankton density. This study found that density is related to both water column depth and time of year, with an increase corresponding to bottom waters and fall months. As desalination plants are increasingly proposed as a solution to the world's growing freshwater crisis, so does their possible negative effects on the environment. The largest concern pertaining to desalination is the briny discharge that can not only affect the growth and development of ichthyoplankton but alter the cues that trigger the transportation of ichthyoplankton into their essential nursery habitat. By using the identified density patterns, we can restrict discharge timing and location, placing the discharge pipe in the upper water column and limiting discharge in fall month when densities are high. These restrictions are needed to minimize the negative effects on fish recruitment and ensure the protection of these economically important fish species.

REFERENCES

- Able, K.W., (2005). A re-examination of fish estuarine dependence: Evidence for connectivity between estuarine and ocean habitats. *Estuarine, Coastal, and Shelf Science* 64, 5-17
- Ackerly, K. L., Roark, K. J., & Nielsen, K. M. (2023). Short-term Salinity Stress During Early Development Impacts the Growth and Survival of Red Drum (*Sciaenops ocellatus*). *Estuaries and Coasts*, 46(2), 541-550.
- Anderson, J. T. (1988). A review of size dependent survival during pre-recruit stages of fishes in relation to recruitment. *Journal of Northwest Atlantic Fishery Science*, 8, 55-66.
- Baccus, D. (1999). The Ecological Condition of Estuaries in the Gulf of Mexico (Report No. 620-R-98-004). U. S. Environmental Protection Agency.
<https://pubs.usgs.gov/publication/70206830>
- Baptista, V., Leitão, F., Morais, P., Teodósio, M. A., & Wolanski, E. (2020). Modelling the ingress of a temperate fish larva into a nursery coastal lagoon. *Estuarine, Coastal and Shelf Science*, 235, 106601.
- Baptista, V., Morais, P., Cruz, J., Castanho, S., Ribeiro, L., Pousão-Ferreira, P., ... & Teodósio, M. A. (2019). Swimming abilities of temperate pelagic fish larvae prove that they may control their dispersion in coastal areas. *Diversity*, 11(10), 185.
- Boehlert, G. W., & Mundy, B. C. (1988). Roles of behavioral and physical factors in larval and juvenile fish recruitment to estuarine nursery areas. In *American Fisheries Society Symposium* (Vol. 3, No. 5, pp. 1-67).
- Bœuf, Gilles, and Patrick Payan. "How should salinity influence fish growth?." *Comparative Biochemistry and Physiology Part C: Toxicology & Pharmacology* 130.4 (2001): 411-423.
- Bromschwig, M. J. (2019). *Feeding Ecology of Ichthyoplankton at a Gulf of Mexico Coastal*

- Inlet*. Master's thesis, Texas A&M University-Corpus Christi 64 pages.
- Brown, C.A., Holt, S.A., Jackson, G.A., Brooks, D.A., & Holt, G.J. (2004). Simulating larval supply to estuarine nursery areas: how important are physical processes to the supply of larvae to the Aransas Pass Inlet? *Fisheries Oceanography* 13, 181–196.
- Brown, C.A., Jackson, G.A., Holt, S.A., & Holt, G.J. (2005). Spatial and temporal patterns in modeled particle transport to estuarine habitat with comparisons to ichthyoplankton settlement patterns. *Estuarine, Coastal and Shelf Science* 64, 33–46.
- Dupavillon, J.L., Gillanders, B.M., 2009. Impacts of seawater desalination on the giant Australian cuttlefish *Sepia apama* in the upper Spencer Gulf, South Australia. *Marine Environmental Research* 67, 207–218.
- Carreon-Martinez, L. B., Wellband, K. W., Johnson, T. B., Ludsin, S. A., & Heath, D. D. (2014). Novel molecular approach demonstrates that turbid river plumes reduce predation mortality on larval fish. *Molecular Ecology*, 23(21), 5366-5377.
- Cuker, B. E., & Watson, M. A. (2002). Diel vertical migration of zooplankton in contrasting habitats of the Chesapeake Bay. *Estuaries*, 25, 296-307.
- Collin, S. P., & Hart, N. S. (2015). Vision and photoentrainment in fishes: the effects of natural and anthropogenic perturbation. *Integrative Zoology*, 10(1), 15-28.
- Erfteimeijer, P. LA, & Lewis III, R. R. R. (2006) "Environmental impacts of dredging on seagrasses: a review." *Marine pollution bulletin* 52.12: 1553-1572.
- Faillottaz, R., Paris, C. B., & Irisson, J. O. (2018). Ichthyoplankton swimming behavior alters dispersal patterns from marine protected areas in the North-Western Mediterranean Sea. *Frontiers in Marine Science*, 5, 97.
- Faria, A., Morais, P., & Chícharo, M. A. (2006). Ichthyoplankton dynamics in the Guadiana

- estuary and adjacent coastal area, South-East Portugal. *Estuarine, Coastal and Shelf Science*, 70(1-2), 85-97.
- Fiksen, Ø., Aksnes, D. L., Flyum, M. H., & Giske, J. (2002). The influence of turbidity on growth and survival of fish larvae: a numerical analysis. In *Sustainable Increase of Marine Harvesting: Fundamental Mechanisms and New Concepts: Proceedings of the 1st Maricult Conference held in Trondheim, Norway, 25–28 June 2000* (pp. 49-59). Springer Netherlands.
- Genner, M. J., Halliday, N. C., Simpson, S. D., Southward, A. J., Hawkins, S. J., & Sims, D. W. (2010). Temperature-driven phenological changes within a marine larval fish assemblage. *Journal of plankton research*, 32(5), 699-708.
- Gibson, R. N., Barnes, M., & Atkinson, R. J. A. (2001). Selective tidal-stream transport of marine animals. *Oceanography and Marine Biology, an Annual Review*, 39, 305-353.
- Hall, Q. A., Curtis, J. M., Williams, J., & Stunz, G. W. (2019). The importance of newly-opened tidal inlets as spawning corridors for adult Red Drum (*Sciaenops ocellatus*). *Fisheries Research*, 212, 48-55.
- Hankin, R. K. S. (2006). Special functions in R: introducing the gsl package. In *R News* (Vol. 6).
- Hays, G. C. (2003). A review of the adaptive significance and ecosystem consequences of zooplankton diel vertical migrations. In *Migrations and Dispersal of Marine Organisms: Proceedings of the 37 European Marine Biology Symposium held in Reykjavík, Iceland, 5–9 August 2002* (pp. 163-170). Springer Netherlands.
- Hernandez, F. J., Hare, J. A., & Fey, D. P. (2009). Evaluating diel, ontogenetic and environmental effects on ichthyoplankton vertical distribution using generalized additive models for location, scale and shape. *Fisheries Oceanography*, 18(4), 224-236.

- Holt, G. J., Holt, S. A., & Arnold, C. R. (1985). Diel periodicity of spawning in sciaenids. *Marine Ecology Progress Series*, 27(1), 7.
- Holt, S. A., Holt, J., & Arnold, C. R. (1990). *Abundance and distribution of larval fishes and shrimps in the Laguna Madre, Texas: a hypersaline lagoon.*
- Holt, G., & Holt, S. (2000). Vertical distribution and the role of physical processes in the feeding dynamics of two larval sciaenids *Sciaenops ocellatus* and *Cynoscion nebulosus*. *Marine Ecology Progress Series* 193, 181–190.
- Ihsanullah, I., Atieh, M.A., Sajid, M., & Nazal, M.K. (2021). Desalination and environment: A critical analysis of impacts, mitigation strategies, and greener desalination technologies. *Science of The Total Environment* 780, 18.
- Irvine K.N., Droppo I.G., Murphy T.P., & Lawson A. (1997); Sediment Resuspension and Dissolved Oxygen Levels Associated with Ship Traffic: Implications for Habitat Remediation. *Water Quality Research Journal*; 32 (2): 421–438.
- Kassambara, A. & Mundt, F. (2020) Factoextra: Extract and Visualize the Results of Multivariate Data Analyses. R Package Version 1.0.7.
<https://CRAN.R-project.org/package=factoextra>
- Kelaher, B. P., Clark, G. F., Johnston, E. L., & Coleman, M. A. (2019). Effect of desalination discharge on the abundance and diversity of reef fishes. *Environmental Science & Technology*, 54(2), 735-744.
- Lampert, W. (1989). The Adaptive Significance of Diel Vertical Migration of Zooplankton. *Functional Ecology*, 3(1), 21–27.
- Lassuy, D. R. (1983). *Species profiles: life histories and environmental requirements (Gulf of Mexico): Gulfmenhaden* (Vol. 11). The Team.

- Lindholm, T., Svartström, M., Spoof, L., & Meriluoto, J. (2001). Effects of ship traffic on archipelago waters off the Långnäs harbour in Åland, SW Finland. *Hydrobiologia*, *444*, 217-225.
- Lowerre-Barbieri, S. K., Ganas, K., Saborido-Rey, F., Murua, H., & Hunter, J. R. (2011). Reproductive timing in marine fishes: variability, temporal scales, and methods. *Marine and Coastal Fisheries*, *3*(1), 71-91.
- Lunt, J., & Smee, D. L. (2014). Turbidity influences trophic interactions in estuaries. *Limnology and Oceanography*, *59*(6), 2002-2012.
- Martin, L., & Esbaugh, A. J. (2021). Osmoregulatory plasticity during hypersaline acclimation in red drum, *Sciaenops ocellatus*. *Journal of Comparative Physiology B*, *191*, 731-740.
- Minello, T.J. (1999). Nekton densities in shallow estuarine habitats of Texas and Louisiana and the identification of essential fish habitat. In *American Fisheries Society Symposium*, **22**, 43-75.
- Miri, R., & Chouikhi, A. (2005). Ecotoxicological marine impacts from seawater desalination plants. *Desalination*, *182*(1-3), 403-410.
- Missimer, T. M., & Maliva, R. G. (2018). Environmental issues in seawater reverse osmosis desalination: Intakes and outfalls. *Desalination*, *434*, 198-215.
- Moustakas, C. T., Watanabe, W. O., & Copeland, K. A. (2004). Combined effects of photoperiod and salinity on growth, survival, and osmoregulatory ability of larval southern flounder *Paralichthys lethostigma*. *Aquaculture*, *229*(1-4), 159-179.
- NOAA: National Marine Fisheries Service & Gulf States Marine Fisheries Commission (2001). SEAMAP Operations Manual for Collection of Data. National Centers for Environmental Information. <https://www.nodc.noaa.gov/archive/arc0090/0150631/1.1/data/0->

data/SEAMAP%20Ops%20MANUAL%202.pdf.

Pankhurst, N. W., & Munday, P. L. (2011). Effects of climate change on fish reproduction and early life history stages. *Marine and Freshwater Research*, 62(9), 1015-1026.

Pepin, P., Robert, D., Bouchard, C., Dower, J. F., Falardeau, M., Fortier, L., ... & Sponaugle, S. (2014). Once upon a larva: revisiting the relationship between feeding success and growth in fish larvae. *ICES Journal of Marine Science*, 72(2), 359-373.

Petersen, K. L., Frank, H., Paytan, A., & Bar-Zeev, E. (2018). Impacts of seawater desalination on coastal environments. In *Sustainable desalination handbook* (pp. 437-463). Butterworth-Heinemann.

Pietrafesa, L. J., Janowitz, G. S., Brown, K. S., Askari, F., Gabriel, C., & Salzillo, L. A. (1988). The invasion of the Red Tide in North Carolina coastal waters.

Pinheiro, J., Bates, D., DebRoy, S., Sarkar, D., & R Core Team. (2021). *nlme: Linear and Nonlinear Mixed Effects Models*. <https://CRAN.R-project.org/package=nlme>

Richards, W. J. (Ed.). (2005). *Early stages of Atlantic fishes: an identification guide for the western central north Atlantic, Two Volume Set* (Vol. 1). CRC Press.

Rao, P., Morrow III, W. R., Aghajanzadeh, A., Sheaffer, P., Dollinger, C., Brueske, S., & Cresko, J. (2018). Energy considerations associated with increased adoption of seawater desalination in the United States. *Desalination*, 445, 213-224.

R Core Team (2021). R: A language and environment for statistical computing. R Foundation for Statistical Computing, Vienna, Austria. URL <https://www.R-project.org/>.

RStudio Team (2020). RStudio: Integrated Development for R. RStudio, PBC, Boston, MA
URL <http://www.rstudio.com/>.

Salonen, M., Urho, L., & Engström-Öst, J. (2009). Effects of turbidity and zooplankton

availability on the condition and prey selection of pike larvae.

- Schieler, B. M., Hale, E. A., & Targett, T. E. (2014). Daily variation in ingress of fall-spawned ichthyoplankton into Delaware Bay in relation to alongshore and along-estuary wind components. *Estuarine, Coastal and Shelf Science*, 151, 141-147.
- Seaberg, W. C. (1988). Observations on inlet flow patterns derived from numerical and physical model studies. In *Am. Fish Soc. Symp.* (Vol. 3, pp. 16-25).
- Shelley, Callyn E., and Darren W. Johnson. "Larval fish in a warming ocean: a bioenergetic study of temperature-dependent growth and assimilation efficiency." *Marine Ecology Progress Series* 691 (2022): 97-114.
- Sims, D. W., Wearmouth, V. J., Genner, M. J., Southward, A. J., & Hawkins, S. J. (2004). Low-temperature-driven early spawning migration of a temperate marine fish. *Journal of Animal Ecology*, 73(2), 333-341.
- Southwick Associates (2006). The 2006 economic benefits of hunting, fishing and wildlife watching in Texas. Southwick Associates Inc., Texas Parks & Wildlife Department.
- Specker, J. L., Schreiber, A. M., McArdle, M. E., Poholek, A., Henderson, J., & Bengtson, D. A. (1999). Metamorphosis in summer flounder: effects of acclimation to low and high salinities. *Aquaculture*, 176(1-2), 145-154.
- Stunz, G. W., Coffey, D. M., & Seemann, F. (2022). *Benchmarking community structure of estuarine-dependent nekton near the Aransas Pass inlet.*
- Teodósio, M.A., Paris, C.B., Wolanski, E., & Morais, P. (2016). Biophysical processes leading to the ingress of temperate fish larvae into estuarine nursery areas: A review. *Estuarine, Coastal and Shelf Science* 183, 187–202.

- Thayer, G. W., Colby, D. R., Kjelson, M. A., & Weinstein, M. P. (1983). Estimates of larval-fish abundance: diurnal variation and influences of sampling gear and towing speed. *Transactions of the American Fisheries Society*, 112(2B), 272-279.
- Tolan, J. M., Holt, S. A., & Onuf, C. P. (1997). Distribution and community structure of ichthyoplankton in Laguna Madre seagrass meadows: potential impact of seagrass species change. *Estuaries*, 20, 450-464.
- Tolan, J. M. (2008). Ichthyoplankton assemblage response to freshwater inflows: A synthesis of five years of ichthyoplankton monitoring within Nueces Bay, Texas. *Bulletin of Marine Science*, 82(3), 275-296.
- Torres, P. (2020, April 13). *U.S. Army Corps of Engineers Awards Dredging Contract For Corpus Christi Ship Channel Improvement Project*. Port of Corpus Christi.
<https://portofcc.com/u-s-army-corps-of-engineers-awards-dredging-contract-for-corpus-christi-ship-channel-improvement-project/>.
- USEPA (US Environmental Protection Agency). (2004). National Pollutant Discharge Elimination System final regulations to establish requirements for cooling water intake structures at Phase II existing facilities, Final Rule. *Federal Register*, 69(131) (9 July 2004), 41575-41693.
- Vega, J. R. M., de Barros, R. P., Chanduvi, J. S., Giugale, M., Cord, L. J., Pessino, C., & Hasan, A. (2011). Human Opportunities in a Global Context: Benchmarking LAC to Other Regions of the World.
- Wang, D. P. (1988). Transport model for water exchange between coastal inlet and the open ocean. In *American Fisheries Society Symposium* (Vol. 3, pp. 9-15).

- Weatherall, T.F., Scheef, L.P., & Buskey, E.J. (2018). Spatial and temporal settlement patterns of blue crab (*Callinectes sapidus* and *Callinectes similis*) megalopae in a drought-prone Texas estuary. *Estuarine, Coastal and Shelf Science* 214, 89–97.
- Wenner, E. L., Knott, D. M., Barans, C. A., Wilde, S., Blanton, J. O., & Amft, J. (2005). Key factors influencing transport of white shrimp (*Litopenaeus setiferus*) post-larvae into the Ossabaw Sound system, Georgia, USA. *Fisheries Oceanography*, 14(3), 175-194.
- Weinstein, M. P., Weiss, S. L., Hodson, R. G., & Gerry, L. R. (1980). Retention of three taxa of postlarval fishes in an intensively flushed tidal estuary, Cape Fear River, North Carolina. *Fishery Bulletin*, 78(2), 419-436.
- Wiseman Jr, W. J., & Dinnel, S. P. (1988). Shelf currents near the mouth of the Mississippi River. *Journal of Physical Oceanography*, 18(9), 1287-1291.
- White, M.L., Chittenden Jr, M.E. (1977). Age determination, reproduction, and population dynamics of the Atlantic croaker, *micropogonias undulatus*. *Fisheries Bulletin*, 75:109–123.
- Whitfield, A. K., Potter, I. C., Neira, F. J., & Houde, E. D. (2023). Modes of ingress by larvae and juveniles of marine fishes into estuaries: From microtidal to macrotidal systems. *Fish and Fisheries*, 24(3), 488-503.
- Zhang, H., Wang, Y., Liang, C., Liu, S., & Xian, W. (2022). Estuarine Ichthyoplankton Studies—A Review. *Frontiers in Marine Science*, 9, 794433.

APPENDIX: STATION CODE DEFINITIONS

Station Code	Station	Time of Day	Tide
PA1DI	Port Aransas (jetties)	Day	In
PA1DO	Port Aransas (jetties)	Day	Out
PA1NI	Port Aransas (jetties)	Night	In
PA1NO	Port Aransas (jetties)	Night	Out
CC1DI	Corpus Christi Channel	Day	In
CC1DO	Corpus Christi Channel	Day	Out
CC1NI	Corpus Christi Channel	Night	In
CC1NO	Corpus Christi Channel	Night	Out
AP1DI	Aransas Pass Channel	Day	In
AP1DO	Aransas Pass Channel	Day	Out
AP1NI	Aransas Pass Channel	Night	In
AP1NO	Aransas Pass Channel	Night	Out
LA1DI	Lydia Ann Channel	Day	In
LA1DO	Lydia Ann Channel	Day	Out
LA1NI	Lydia Ann Channel	Night	In
LA1NO	Lydia Ann Channel	Night	Out